

# New Calcium-Selective Smart Contrast Agents for Magnetic Resonance Imaging

Kirti Dhingra Verma,<sup>[a, b]</sup> Attila Forgács,<sup>[c]</sup> Hyounsoo Uh,<sup>[d]</sup> Michael Beyerlein,<sup>[a]</sup> Martin E. Maier,<sup>[e]</sup> Stéphane Petoud,<sup>[d, f]</sup> Mauro Botta,<sup>[c]</sup> and Nikos K. Logothetis<sup>[a, g]</sup>

**Abstract:** Calcium plays a vital role in the human body and especially in the central nervous system. Precise maintenance of  $\text{Ca}^{2+}$  levels is very crucial for normal cell physiology and health. The deregulation of calcium homeostasis can lead to neuronal cell death and brain damage. To study this functional role played by  $\text{Ca}^{2+}$  in the brain noninvasively by using magnetic resonance imaging, we have synthesized a new set of  $\text{Ca}^{2+}$ -sensitive smart contrast agents (CAs). The agents were found to be highly selective to  $\text{Ca}^{2+}$  in the presence of other competitive anions and cations in buffer and in physiological fluids. The structure of CAs comprises  $\text{Gd}^{3+}$ -DO3A (DO3A = 1,4,7-tris(carb-

oxymethyl)-1,4,7,10-tetraazacyclododecane) coupled to a  $\text{Ca}^{2+}$  chelator *o*-amino phenol-*N,N,O*-triacetate (APTRA). The agents are designed to sense  $\text{Ca}^{2+}$  present in extracellular fluid of the brain where its concentration is relatively high, that is, 1.2–0.8 mM. The determined dissociation constant of the CAs to  $\text{Ca}^{2+}$  falls in the range required to sense and report changes in extracellular  $\text{Ca}^{2+}$  levels followed by an increase in neural activity. In buffer, with the addition of  $\text{Ca}^{2+}$  the

**Keywords:** calcium • gadolinium • magnetic resonance imaging • relaxivity • sensors

increase in relaxivity ranged from 100–157%, the highest ever known for any  $T_1$ -based  $\text{Ca}^{2+}$ -sensitive smart CA. The CAs were analyzed extensively by the measurement of luminescence lifetime measurement on  $\text{Tb}^{3+}$  analogues, nuclear magnetic relaxation dispersion (NMRD), and  $^{17}\text{O}$  NMR transverse relaxation and shift experiments. The results obtained confirmed that the large relaxivity enhancement observed upon  $\text{Ca}^{2+}$  addition is due to the increase of the hydration state of the complexes together with the slowing down of the molecular rotation and the retention of a significant contribution of the water molecules of the second sphere of hydration.

## Introduction

Calcium plays an important dual role as a carrier of electric current and as a second messenger in the brain. Several proteins such as calmodulin, calcineurin, and synaptotagmin affect the role of  $\text{Ca}^{2+}$  in neural signal transduction. Following activation of these proteins by an influx of  $\text{Ca}^{2+}$ , a cascade of events takes place, which further targets a wide variety of enzymes.<sup>[1]</sup> Since the action of  $\text{Ca}^{2+}$  is mediated by such a diverse array of protein and countless other  $\text{Ca}^{2+}$ -

modulated enzymes, its effects on neural activity are much more diverse than for any other second messenger.<sup>[2]</sup>

The influx of  $\text{Ca}^{2+}$  from extracellular space is maintained by channels in plasma membrane, which tightly maintains an enormous chemical gradient of 15000–40000:1, from outside to inside.<sup>[1b,3]</sup> Studies performed by using ion-selective micropipettes have shown that during normal brain activity, the extracellular  $\text{Ca}^{2+}$  concentrations ( $[\text{Ca}^{2+}]_o$ ) decreases by  $\approx 15\%$ . However, during maximal stimulation it can decrease up to  $\approx 30\%$ , whereas under traumatic events such as

[a] Dr. K. D. Verma, M. Beyerlein, Prof. Dr. N. K. Logothetis  
Max Planck Institute for Biological Cybernetics  
Dept. of Physiology of Cognitive Processes  
72076 Tübingen (Germany)  
E-mail: kirtil601@googlemail.com  
nikos.logothetis@tuebingen.mpg.de

[b] Dr. K. D. Verma  
Present address: Case NRCR Center for Imaging Research  
Dept. of Radiology, Case Western Reserve University  
Cleveland, OH (USA)

[c] A. Forgács, Prof. Dr. M. Botta  
Dipartimento di Scienze e Innovazione Tecnologica  
Università del Piemonte Orientale “Amedeo Avogadro”  
Viale Teresa Michel 11, 15121 Alessandria (Italy)

[d] Dr. H. Uh, Prof. Dr. S. Petoud  
Department of Chemistry, University of Pittsburgh  
Pittsburgh, PA (USA)

[e] Prof. Dr. M. E. Maier  
Institut für Organische Chemie  
Eberhard Karls Universität Tübingen  
72076 Tübingen (Germany)

[f] Prof. Dr. S. Petoud  
Centre de Biophysique Moléculaire  
CNRS UPR 4301, Rue Charles Sadron  
45071 Orléans Cedex 2 (France)

[g] Prof. Dr. N. K. Logothetis  
Imaging Science and Biomedical Engineering  
University of Manchester, Manchester (UK)

 Supporting information for this article is available on the WWW under <http://dx.doi.org/10.1002/chem.201300169>.

epileptic seizures and terminal anoxia it can decrease up to  $\approx 90\%$ .<sup>[4]</sup> The fluctuations in  $\text{Ca}^{2+}$  concentrations ( $[\text{Ca}^{2+}]_o$ ) are therefore considered to be a significant factor in determining the nervous system function. The development of fluorescent dyes has greatly helped to our understanding of this critical role played by  $\text{Ca}^{2+}$ .<sup>[5]</sup> However the current limitation of the depth of penetration of optical imaging techniques and the production of side products resulting from the photobleaching of the dyes when exposed to light narrows the applications of this modality to only superficial regions.

Magnetic resonance imaging (MRI) on the other hand is an imaging modality that provides excellent three-dimensional spatial resolution down to the  $10\ \mu\text{m}$  range, whole-body coverage, and the opportunity to measure additional physiological parameters. However, it is a technique that has relatively low sensitivity and that therefore requires the aid of external agents, known as contrast agents (CAs), for example,  $\text{Gd}^{3+}$  chelates. The  $\text{Gd}^{3+}$ -based CAs accelerates the longitudinal and transverse relaxation rate of water protons and hence enhances the image contrast by means of spatially selective signal-increases. Such  $\text{Gd}^{3+}$  based CAs produces a positive contrast in a  $T_1$ -weighted MRI image.<sup>[6]</sup>

Currently, another class of CAs known as smart contrast agents (SCAs) is being explored and catching the attention of researchers in the field of CAs for MRI. These agents are designed in a way that they enhance the signal-to-noise ratio in the MRI image only when triggered by a physiological event such as changes in the metal ion ( $\text{Ca}^{2+}$ ,  $\text{Zn}^{2+}$ ,  $\text{Cu}^{2+}$ , etc.) concentrations,<sup>[7]</sup> enzyme activity,<sup>[8]</sup> and so on. To this end, Li et al. have reported a  $\text{Gd}^{3+}$ -based CA, Gd-DOPTA, which is sensitive to  $\text{Ca}^{2+}$  in the  $0.1\text{--}10\ \mu\text{M}$  range ( $K_d = 0.98\ \mu\text{M}$ ).<sup>[7c]</sup> Given its low dissociation constant, it can neither be used to detect extracellular  $\text{Ca}^{2+}$  fluctuations ( $1.2\ \text{mM}$  to  $0.8\ \text{mM}$ ) nor intracellular  $\text{Ca}^{2+}$  because it lacks transport ability to cross the cell membrane barrier. Along these lines, we have published earlier a new class of SCA based on the structure of APTRA (*o*-amino phenol-*N,N,O*-triacetate) linked to Gd-DO3A unit.<sup>[7b]</sup> The choice of APTRA was made due to its low chelating affinity with dissociation constant  $20\text{--}25\ \mu\text{M}$ . High affinity chelators such as 1,2-bis(*o*-aminophenoxy) ethane *N,N,N',N'*-tetraacetic acid (BAPTA) as incorporated in the structure of DOPTA, with dissociation constant  $0.1\text{--}0.4\ \mu\text{M}$  are not suitable when the  $[\text{Ca}^{2+}]$  increases above  $1\ \mu\text{M}$ .

Gd-DOPTRA showed excellent sensitivity to  $\text{Ca}^{2+}$  resulting in  $\approx 100\%$  increase in the relaxivity,  $r_{1p}$ . The relaxivity response in complex biological fluids such as artificial cerebrospinal fluid (ECSF) and artificial extracellular matrix (AECM) was moderate, 27 and 36%, respectively. The complexes once formed were highly stable; however, very slow hydrolysis of one acetate arm was observed during the loading of  $\text{Ln}^{3+}$  ions to the macrocyclic ligand similarly to a previous report published by another group.<sup>[9]</sup> The next step was to improve this stability issue and increase the relaxivity response in complex biological fluids. With these objectives in mind we designed several new CAs based on the APTRA

series. The introduced structural changes resulted in the increase of the stability in respect to the release of acetate arm. The maxima of relaxivity changes obtained were larger, 157% with improved specificity to  $\text{Ca}^{2+}$  in complex biological fluids. As of today, and to the best of our knowledge, the changes observed are the highest of any  $\text{Ca}^{2+}$ -sensitive SCA reported. The turn-on response of the agents to  $\text{Ca}^{2+}$  was extensively investigated in by the measurement of luminescence lifetime measurement on  $\text{Tb}^{3+}$  analogues, of dissociation constant determination, nuclear magnetic relaxation dispersion (NMRD), and  $^{17}\text{O}$  NMR transverse relaxation and shift experiments.

## Results and Discussion

Four different agents were designed and synthesized, Gd-DOPTRA-(2–5), which share structural similarity to our previously published molecule, Gd-DOPTRA-1 (Figure 1).<sup>[7b]</sup> We sought for higher  $\text{Ca}^{2+}$ -dependent relaxivity changes and improved selectivity of the agents toward  $\text{Ca}^{2+}$  in complex biological media with stability toward release of acetate arm (the Supporting Information, Figure S1). With respect to the stability limitation, we hypothesized that it might be due to the lone pair on the oxygen in the linker connecting the macrocycle to the aromatic ring of the APTRA unit. We therefore designed Gd-DOPTRA-2 that does not contain any oxygen in the linker and has overall a shorter linker consisting of one carbon unit. The complexes formed with this ligand were found to be stable but did not show any change in the relaxivity in response to  $\text{Ca}^{2+}$  addition (see discussion later). The stability of the Gd-DOPTRA-2 complex proved however that the instability of Gd-DOPTRA-1 was due to the presence of the oxygen atom in the linker directly connected to the aromatic ring of the APTRA unit (the details of this mechanism are under investigation). This result prompted us to design Gd-DOPTRA-3, featuring a carbon unit between the aromatic ring and the oxygen of the linker that prevent their direct connection. This structure served as the base to other designed agents. Further changes were made in the phenolic coordinating arm of Gd-DOPTRA-3 to improve its  $\text{Ca}^{2+}$ -specific relaxivity response. A report published by Tsien and co-workers discussed the possible structure modification of APTRA to make it much more  $\text{Ca}^{2+}$  selective and with better rejection ability to  $\text{Mg}^{2+}$ .<sup>[10]</sup> As discussed in their paper, the best results were obtained by converting the acetate group on the phenolic oxygen to a morpholino amide group. Similar modification was incorporated in the Gd-DOPTRA-4, whereas the modification of Gd-DOPTRA-5 consisted of an extended etheral linkage similar to what is present in BAPTA (a selective  $\text{Ca}^{2+}$  chelator). All of these agents were systematically analyzed for their  $\text{Ca}^{2+}$  specific relaxivity enhancement from simple buffer solution to complex biological media.

**Synthesis:** The synthesis of Gd-DOPTRA-2 started with commercially available 3-methoxy-2-nitrobenzaldehyde

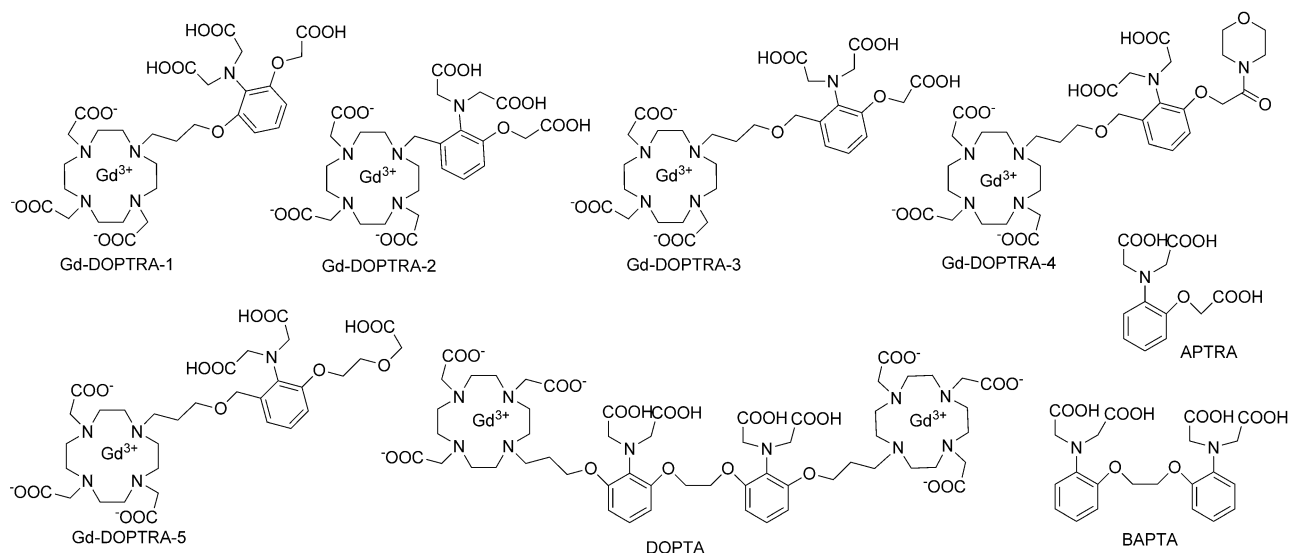
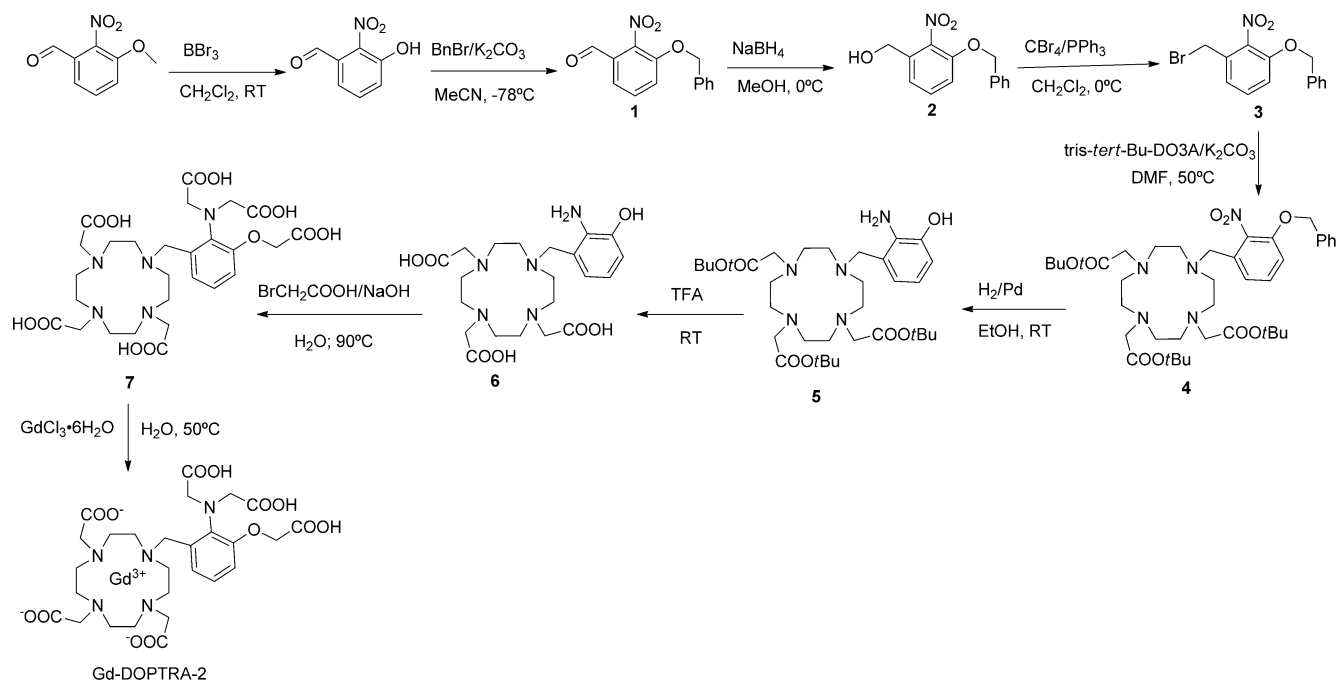


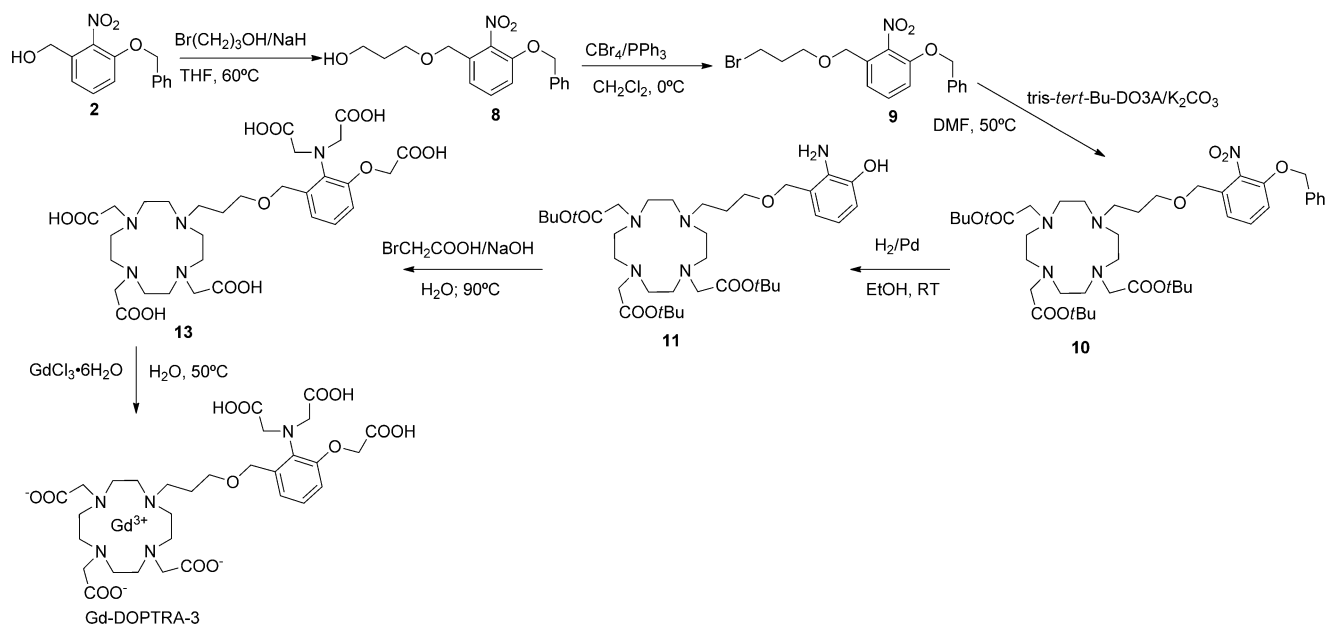
Figure 1. Structure of DOPTRA-based contrast agents compared to the structures of DOPTA, BAPTA, and APTRA.

(Scheme 1). The methyl ether group was hydrolyzed with boron tribromide followed by alkylation with benzyl bromide to give **1**. The reduction of the aldehyde group in **1** was carried out with sodium borohydride to give alcohol **2**, which was then brominated with carbon tetrabromide and triphenyl phosphine to afford **3**. Tris-*tert*-Bu-DO3A was synthesized according to the procedure published earlier<sup>[11]</sup> and was then used for alkylation reaction with **3** to yield **4**. The reduction of the nitro group and removal of the benzyl group was simultaneously carried out on **4** through a palladium-catalyzed hydrogenation to obtain **5**. The saponification

of *tert*-butyl esters in **5** was carried out with trifluoroacetic acid (TFA) followed by reverse phase (RP)-HPLC purification using the method described in the Experimental Section. The aromatic amino group and the phenolic group in **5** were simultaneously alkylated with bromoacetic acid to give ligand **6**. This product was purified by RP-HPLC and then metalated with  $\text{GdCl}_3 \cdot 6\text{H}_2\text{O}$  (or  $\text{TbCl}_3 \cdot 6\text{H}_2\text{O}$ ) (1:1.1) in water at 50°C and pH 7 for 24 h to give Gd-DOPTRA-2 (and  $\text{Tb}^{3+}$  for the corresponding analogue). Obtained complexes were then treated with chelex 100 to remove any uncomplexed  $\text{Gd}^{3+}$ . The synthesis of Gd-DOPTRA-3 began



Scheme 1. The synthetic scheme of Gd-DOPTRA-2.



Scheme 2. The synthetic scheme for Gd-DOPTRA-3.

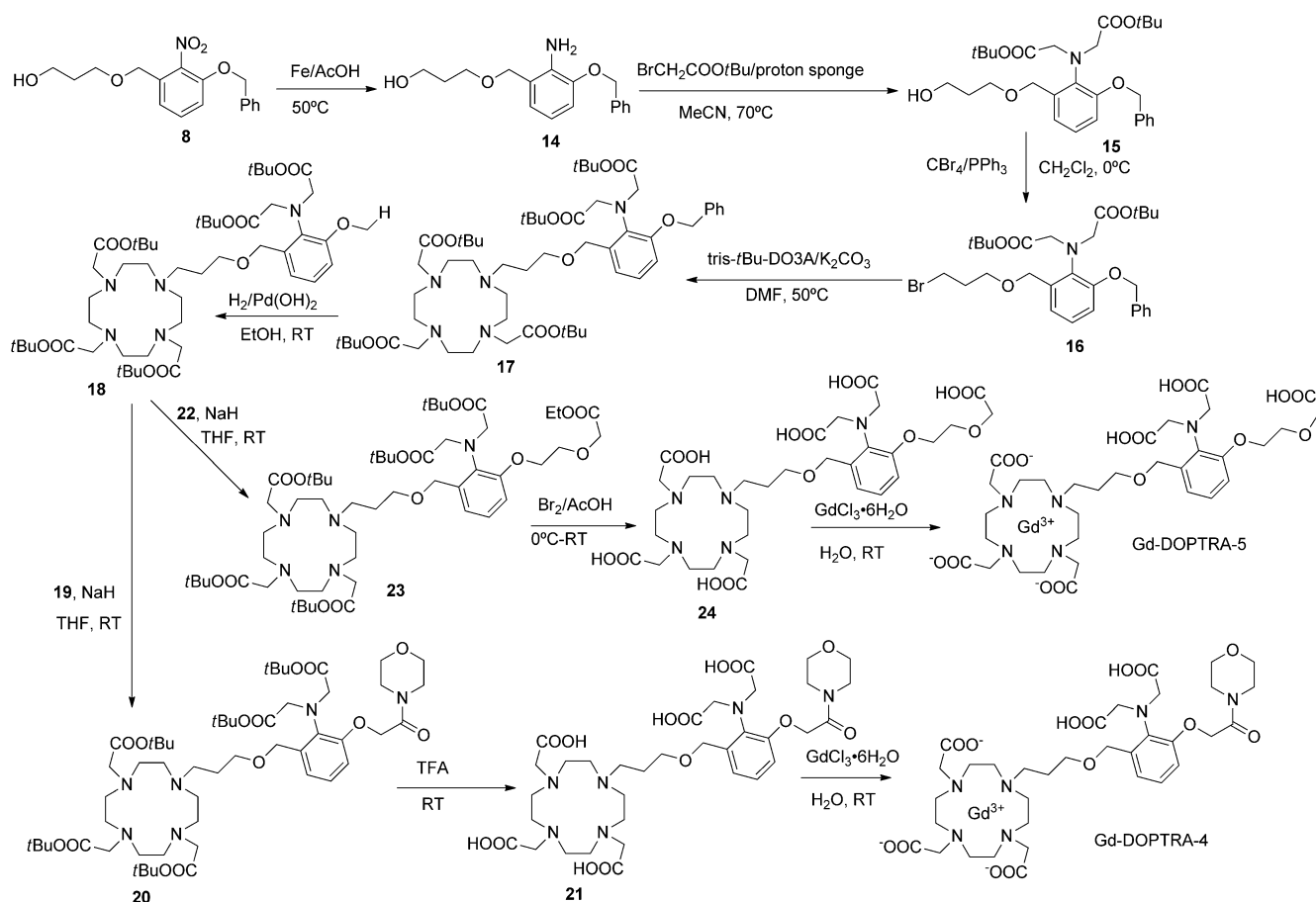
with the precursor **2**, in which the alcohol group was alkylated with bromopropanol using sodium hydride as the base to give **8** (Scheme 2). The final agent Gd-DOPTRA-3 was obtained from **8** in a manner similar to that of Gd-DOPTRA-2 starting from the precursor **2**. Gd-DOPTRA-4 and -5 were prepared according to a different synthetic procedure, because they require selective alkylation at the phenolic group with morpholino precursor for Gd-DOPTRA-4 and ethyl 2-(2-bromoethoxy)acetate precursor for Gd-DOPTRA-5. The synthesis began with the precursor **8**, in which the aromatic nitro group was reduced with iron-acetic acid to give **14** (Scheme 3). The aromatic amine in **14** was treated with *tert*-butyl bromoacetate using a proton sponge as the base to yield **15**. The alcohol group in **14** was alkylated with carbon tetrabromide to afford **16**, which was then used to alkylate *tris-tert*-Bu-DO3A in DMF to give **17**. The benzyl group was then removed under hydrogenation conditions using palladium hydroxide as the catalyst to give **18**. This compound served as the common precursor for Gd-DOPTRA-4 and -5. The morpholine precursor **19** (Scheme 4) was synthesized using bromoacetyl bromide and morpholine at  $0^\circ\text{C}$  using ice bath. This intermediate was used to alkylate the phenolic group in **18** using sodium hydride as the base to afford **20**. The *tert*-butyl esters were hydrolyzed by using TFA followed by RP-HPLC purification to give the ligand **21**. This reagent was metalated to obtain Gd-DOPTRA-4 in a similar manner as previously described. For Gd-DOPTRA-5, precursor **22** was prepared by Rh(II)-catalyzed O-alkylation of bromoethanol with ethyl diazoacetate (Scheme 3).<sup>[12]</sup> The precursor **18** was alkylated by **22** using sodium hydride as base followed by saponification of esters in one pot to furnish ligand **24** (Scheme 3). The metalation with  $\text{GdCl}_3 \cdot 6\text{H}_2\text{O}$  (or  $\text{TbCl}_3 \cdot 6\text{H}_2\text{O}$ ) was performed as described previously to obtain the final agent Gd-DOPTRA-5.

**Relaxivity study:** The relaxivity measurements of the CAs in absence or presence of  $\text{Ca}^{2+}$  were performed at 400 MHz,  $25^\circ\text{C}$ , and pH 7.4 (KMOPS buffer, MOPS=3-(*N*-morpholino)propanesulfonic acid). The longitudinal relaxivity was calculated from Equation (1), in which  $T_{1\text{obs}}$  is the measured longitudinal relaxation time,  $T_{1\text{d}}$  is the diamagnetic contribution of the solvent and  $T_{1\text{p}}$  is the paramagnetic contribution caused by the CA.  $1/T_{1\text{p}}$  is directly proportional to the concentration of CA  $[\text{Gd}]$  [Eq. (2)].

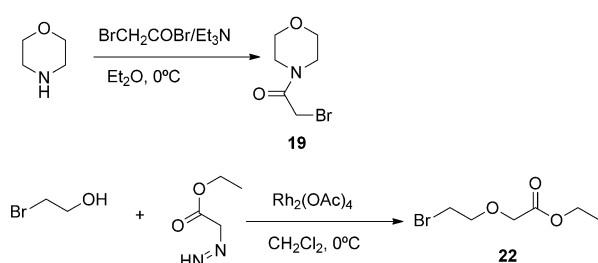
$$\frac{1}{T_{1\text{obs}}} = \frac{1}{T_{1\text{d}}} + \frac{1}{T_{1\text{p}}} \quad (1)$$

$$\frac{1}{T_{1\text{obs}}} = \frac{1}{T_{1\text{d}}} + r_1[\text{Gd}] \quad (2)$$

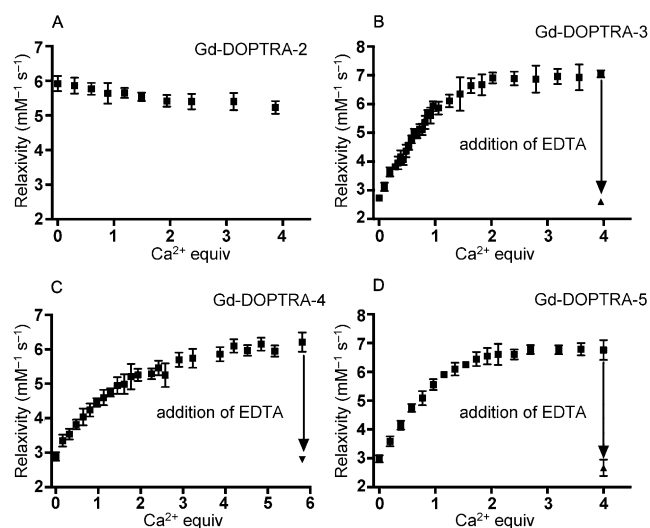
The initial  $r_1$  of the Gd-DOPTRA-2 was found to be  $6.0 \text{ mM}^{-1} \text{ s}^{-1}$ , which is approximately 1.7 times larger than the initial relaxivity for Gd-DOPTRA-1. The addition of  $\text{Ca}^{2+}$  to the buffered solution of the complex did not result in an increase in relaxivity (Figure 2A). The high initial relaxivity value that does not vary in response to  $\text{Ca}^{2+}$  addition is indicative of high hydration state of Gd-DOPTRA-2. It also suggests that the short linker (as in Gd-DOPTRA-2) is inefficient and that the linker incorporating three carbons and one oxygen unit (as in Gd-DOPTRA-1) is more favorable. It allows, in the absence of  $\text{Ca}^{2+}$ , the efficient blocking of access of water molecules to  $\text{Gd}^{3+}$  by intramolecular ligation and provides a desired flexibility and binding properties in presence of  $\text{Ca}^{2+}$ . The structure of Gd-DOPTRA-3 does consist of a similar linker but with an extra carbon unit introduced to bring additional stability to the complex. As expected, Gd-DOPTRA-3 was found to be stable toward a slow release of aminoacetate arm. The relaxivity in ab-



Scheme 3. The synthetic scheme for Gd-DOPTRA-(4 and -5).

Scheme 4. The synthetic scheme for the precursors **19** and **22**.

sence of Ca<sup>2+</sup> was found to be 2.7 mM<sup>-1</sup>s<sup>-1</sup> compared with 3.5 mM<sup>-1</sup>s<sup>-1</sup> for Gd-DOPTRA-1. With the addition of Ca<sup>2+</sup>, the *r*<sub>1</sub> value increased with the saturation limit observed at 7.0 mM<sup>-1</sup>s<sup>-1</sup> (molar ratio ≥ 2). This accounted for an increase of 157%, which is 60% higher compared with Gd-DOPTRA-1 (Figure 2B). A low initial *r*<sub>1</sub> implies a tighter coordination of the pendant arm to Gd<sup>3+</sup> in absence of Ca<sup>2+</sup>, which is a highly desirable property for a smart contrast agent. A larger change in relaxivity suggests that the new linker in Gd-DOPTRA-3 has an optimum flexibility and length to allow tighter coordination of aminoacetate arms to Gd<sup>3+</sup> and at the same time provide the structural stability to

Figure 2. Ca<sup>2+</sup>-dependent relaxivity profile of Gd-DOPTRA-(2–5) in KMOPS buffer, pH 7.4, 400 MHz, and 298 K.

the agent. Based on these optimized linkers, we synthesized two additional agents, Gd-DOPTRA-4 and -5. Compared with Gd-DOPTRA-3, the variation of the initial *r*<sub>1</sub> of Gd-DOPTRA-4 and -5 is small, as an indication of similar effi-

ciency of the pendant arms for the displacement of coordinated water molecules and coordination to  $Gd^{3+}$ . The addition of  $Ca^{2+}$  to the buffered solution of Gd-DOPTRA-4 elicited the expected enhancement in relaxivity. A final  $r_1$  value of  $6.0\text{ mm}^{-1}\text{ s}^{-1}$  was obtained, which corresponds to a 114% increase (Figure 2C). A comparatively slow increase of  $r_1$  was observed with saturation at about three equivalents of  $Ca^{2+}$ . This trend indicates that the agent has a lower binding affinity to  $Ca^{2+}$ , which is expected because of the nature of the pendant arm, a combination of morpholino amide and aminoacetates groups. On the other hand, a similar behavior to Gd-DOPTRA-3 was shown by Gd-DOPTRA-5, which presents a pendant arm combining aminoacetate groups and ethereal oxygen atoms, similar to what has been observed for the BAPTA structure. The relaxivity in absence of  $Ca^{2+}$  was observed to be  $2.6\text{ mm}^{-1}\text{ s}^{-1}$  and rose to  $5.9\text{ mm}^{-1}\text{ s}^{-1}$  in presence of  $Ca^{2+}$ , corresponding to a 125% increase (Figure 2D). All agents were also tested for their ability to bind reversibly to  $Ca^{2+}$ . When ethylenediamine tetracetic acid (EDTA) was added to the CA solution saturated with  $Ca^{2+}$ , the relaxivity dropped back to the values observed for the  $Ca^{2+}$ -free solutions. This observation shows that the complexation of pendant arms of the CA to  $Ca^{2+}$  is reversible, a desired property to monitor increase and decrease of  $[Ca^{2+}]_o$  levels due to decrease and increase of neural activity, respectively.

**Mechanism of relaxivity enhancement:** To analyze the mechanism of  $Ca^{2+}$  sensitivity of the agents, we carried out a detailed relaxometric study to assess the role of the various parameters affecting the relaxivity of the CAs in presence and absence of  $Ca^{2+}$ . According to the Solomon–Bloembergen–Morgan theory, the paramagnetic relaxation rate  $1/T_{1p}$  or  $R_{1p}$ , describes the effect of the paramagnetic ion-solvent molecules magnetic interaction and includes contributions of water molecules belonging to the different hydration states: first- (IS), second- (SS) and outer-hydration sphere (OS).<sup>[6,13]</sup>

$$R_{1p} = R_{1p}^{IS} + R_{1p}^{SS} + R_{1p}^{OS} \quad (3)$$

The relaxivity of the Gd complex is simply defined as the increment of the paramagnetic water proton relaxation rate per unit concentration,  $r_1 = R_{1p}/[C_{tot}]$ . A large number of parameters (water exchange rate,  $k_{ex} = 1/\tau_M$ ; rotational correlation time,  $\tau_R$ , electronic relaxation times,  $1/T_{1,2e}$ ; Gd-proton distance,  $r_{GdH}$ ; hydration number,  $q$ ) influences the relaxivity. Normally, the largest contribution to the relaxivity of  $Gd^{3+}$  complexes with  $q \geq 1$  is provided by the inner-sphere (IS) term:

$$r_1^{IS} = p_M / (T_{1M} + \tau_M) \quad (4)$$

in which  $p_M$  is the molar fraction of inner-sphere water molecules ( $p_M = ([GdL]q)/55.6$ ),  $T_{1M}$  is the longitudinal nuclear magnetic relaxation time of the bound water protons and  $\tau_M$

( $\tau_M = 1/k_{ex}$ ) is the mean residence lifetime of the coordinated water molecule(s). We performed luminescence lifetime measurement on the  $Tb^{3+}$  analogue of CAs to determine the hydration number  $q$  value and a combined relaxometric study consisting of the acquisition of variable temperature  $^{17}O$  NMR data and  $^1H$  relaxivity data as the function of the magnetic field strength (NMRD profile) to ascertain the role played by the molecular parameters in determining the relaxivity of CAs and its enhancement in presence of  $Ca^{2+}$ .

**Luminescence lifetime measurement:** Luminescence lifetime measurements were performed on the  $Tb^{3+}$  analogues of CAs in  $H_2O$  and  $D_2O$ . The  $\tau_{H_2O}$  and  $\tau_{D_2O}$  values calculated on the experimental data measured for all the CAs is summarized in Table 1. The lifetimes observed in aqueous media are observed to be shorter than in the deuterated media. This result is attributed to the non-radiative quench-

Table 1. Luminescence lifetimes and estimated  $q$  values for  $Tb^{3+}$  analogues of CAs (KMOPS, pH 7.4).

CAs	Without $Ca^{2+}$		$q$	With $Ca^{2+}$		$q$
	$\tau_{H_2O}$ [ms]	$\tau_{D_2O}$ [ms]		$\tau_{H_2O}$ [ms]	$\tau_{D_2O}$ [ms]	
Gd-DOPTRA-2	$1.508 \pm 0.003$	$2.335 \pm 0.005$	0.9	$1.144 \pm 0.006$	$1.514 \pm 0.003$	0.8
Gd-DOPTRA-3	$1.848 \pm 0.004$	$2.235 \pm 0.005$	0.2	$1.165 \pm 0.003$	$1.654 \pm 0.004$	1.0
Gd-DOPTRA-4	$1.800 \pm 0.004$	$2.144 \pm 0.005$	0.1	$0.863 \pm 0.004$	$1.193 \pm 0.007$	1.3
Gd-DOPTRA-5	$1.863 \pm 0.003$	$2.390 \pm 0.004$	0.3	$1.261 \pm 0.002$	$1.876 \pm 0.003$	1.0

ing due to the overtones of the vibrations of O–H oscillators that deactivates the luminescence from the lanthanide metal ion. O–D oscillators result in the need of higher energy (larger number of overtones) to interact with the excited emissive state of  $Tb^{3+}$  and therefore quenches the  $Tb^{3+}$  luminescence with a lower efficiency. The number of inner-sphere water molecules ( $q$ ) was calculated from the revised Equation of Beeby, Parker, et al. This Equation includes a correction for the contribution of second sphere water molecules [Eq. (5)].<sup>[14]</sup>

$$q = A \times (\tau_{H_2O}^{-1} - \tau_{D_2O}^{-1} - B) \quad (5)$$

in which  $A = 5$  and  $B = 0.06$  for  $Tb^{3+}$ .

For Gd-DOPTRA-(3–5) the value of  $q$  is close to zero in absence of  $Ca^{2+}$ . In presence of  $Ca^{2+}$ , the value increases to  $q \approx 1$ . These values are in agreement with the relaxivity data that is, an increase in hydration number resulted in an increase in relaxivity. Luminescence lifetime results for Gd-DOPTRA-2 are also in line with the corresponding relaxivity data. The high initial relaxivity observed for Gd-DOPTRA-2 (1.7 times compared with the other CAs) corresponds to its higher (close to one) hydration number. The complete absence of change in relaxivity upon addition of  $Ca^{2+}$  is also reflected in its constant  $q$  value in absence and in presence of  $Ca^{2+}$ . The equilibrium shifts to the right in presence of  $Ca^{2+}$  for Gd-DOPTRA-(3–5), whereas it is

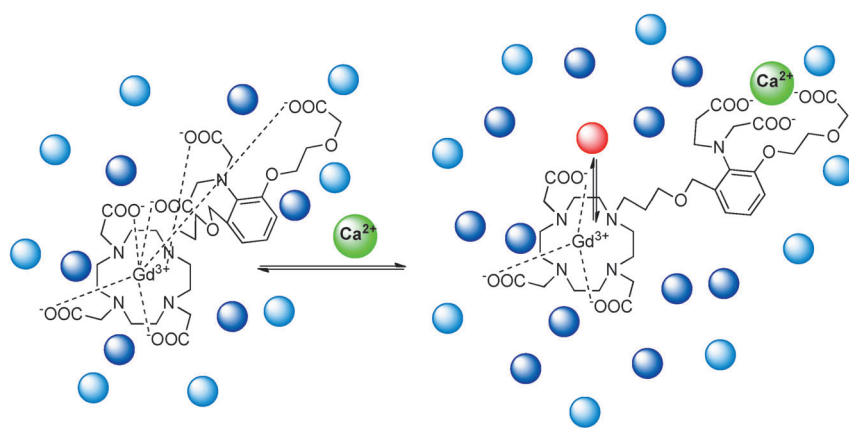


Figure 3. The reversible binding of Gd-DOPTRA-(3–5) to  $\text{Ca}^{2+}$  (shown here with Gd-DOPTRA-5 structure). Dark-blue and light-blue circles indicate second-sphere and outer-sphere contributions to observed relaxivity. The red circle indicates an inner-sphere water molecule directly in contact with  $\text{Gd}^{3+}$ .

initially located toward the right for Gd-DOPTRA-2 (Figure 3). The relaxivity changes however are much higher than what is indicated by their corresponding hydration number. This observation is likely due the fact that the observed total change in relaxivity is due to the collective effect of changes in the inner-sphere- as well as outer- and second-sphere solvation effects [Eq. (3)].

**Relaxometric measurements:** Variable temperature  $^{17}\text{O}$  NMR transverse relaxation rate ( $R_2=1/T_2$ ) and shift ( $\Delta\omega$ ) data and  $^1\text{H}$  NMRD profiles were acquired and analyzed. For GD-DOPTRA-(3–5), the NMRD profiles were recorded in absence and presence of  $\text{Ca}^{2+}$  (Figure 8).

**NMRD and  $^{17}\text{O}$  NMR spectroscopy:** It is well established that in the case of low-molecular-weight  $\text{Gd}^{3+}$  chelates, the IS contribution at high magnetic field strength ( $>0.2$  T) is largely determined by the fast molecular tumbling rate in solution, characterized by the rotational correlation time  $\tau_R$  that assumes values in the range of about 50–200 ps. As a consequence, the NMRD profiles of small  $\text{Gd}^{3+}$  chelates are characterized by a typical shape: a region of constant relaxivity in the frequency range  $\approx 0.01$ –1 MHz, a dispersion at about 5–8 MHz, and another plateau at higher frequencies.<sup>[6,13]</sup> The NMRD profiles of Gd-DOPTRA-2 measured at 298 and 310 K reproduce well this trend (Figure 4).

The  $r_1$  value for Gd-DOPTRA-2 assumes the value of  $8.8 \text{ mm}^{-1}\text{s}^{-1}$  at 20 MHz and 298 K. This value appears sensibly higher than expected for a monohydrated Gd-DOTA-like complex of similar molecular size.<sup>[13a]</sup> As previously observed, a significant SS contribution is likely to be present in mono-aqua Gd complexes functionalized with hydrophilic pendant groups.<sup>[15]</sup> Variable temperature  $R_2$  and chemical shift ( $\Delta\omega$ )  $^{17}\text{O}$  NMR measurements were carried out at 11.7 T on a 12.8 mm solution of the CAs in  $^{17}\text{O}$ -enriched water. The data were analyzed using Swift–Connick set of Equations that provide accurate estimates of the water exchange lifetime,  $\tau_M$  (Figure 5).

In the best-fit procedure, the following parameters were adjusted:  $\tau_M$ ,  $\Delta H_M^\ddagger$ ,  $A/\hbar$ ,  $\Delta^2$  and  $\tau_V$ . The activation energy for the temperature dependence of  $\tau_V$ ,  $E_V$ , was fixed to  $1 \text{ kJ mol}^{-1}$  e because it tends otherwise to assume unrealistic large values. In addition, based on the large collection of data available, some of the parameters were allowed to vary only within a reasonable interval of values:  $\Delta^2$  ( $1$ – $10 \times 10^{19} \text{ s}^{-2}$ ),  $\tau_V$  (1–30 ps),  $A/\hbar$  ( $3$ – $4 \times 10^6 \text{ rad s}^{-1}$ ).<sup>[13b,16]</sup>

The hydration state of the complex plays a relevant role in defining its relaxivity as it

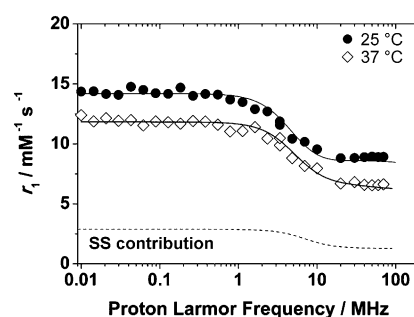


Figure 4.  $^1\text{H}$  NMRD profiles of Gd-DOPTRA-2 recorded at 25 and 37 °C. The lines represent the fit of the experimental data as explained in the text. The dashed line represents the estimated SS contribution to the relaxivity at 25 °C.

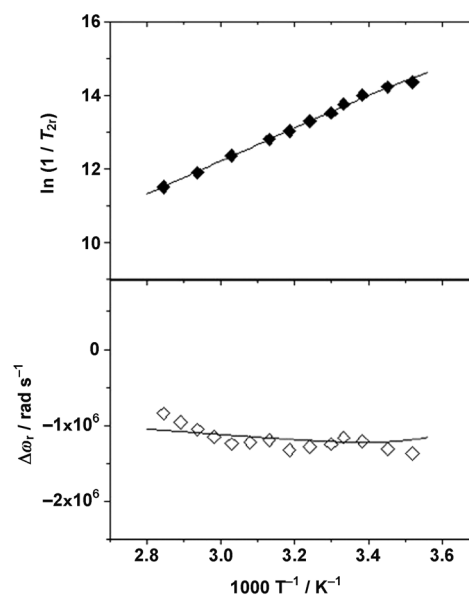


Figure 5. Temperature dependence of the reduced transverse  $^{17}\text{O}$  relaxation rates (top) and chemical shifts (bottom) of a solution of Gd-DOPTRA-2 at 11.75 T and neutral pH.

Table 2. Parameters obtained from the analysis of  $^1\text{H}$  NMRD profiles and  $^{17}\text{O}$  NMR data (11.7 T) for the  $\text{Gd}^{3+}$  complexes of DOPTRA-(2–5).<sup>[a]</sup>

Parameters	2	3	3 + $\text{Ca}^{\text{II}}$	4	4 + $\text{Ca}^{\text{II}}$	5	5 + $\text{Ca}^{\text{II}}$	DOTA <sup>[c]</sup>
$^{20}\tau_1^{298}$ [ $\text{mM}^{-1}\text{s}^{-1}$ ]	8.8	4.5	9.0	4.2	8.3	4.6	10.5	4.7
$\Delta^2$ [ $10^{19}\text{s}^{-2}$ ]	$4.1 \pm 0.4$	$3.9 \pm 0.3$	$3.6 \pm 0.2$	$5.4 \pm 0.2$	$5.6 \pm 0.3$	$6.0 \pm 0.3$	$4.7 \pm 0.2$	1.6
$\tau_V^{298}$ [ps]	$21 \pm 2$	$28 \pm 3$	$28 \pm 2$	$22 \pm 2$	$23 \pm 1$	$21 \pm 2$	$26 \pm 3$	11
$\tau_M^{298}$ [ns]	$14 \pm 1$	–	$10 \pm 1$	–	$11 \pm 2$	–	$34 \pm 4$	244
$\tau_R^{298}$ [ps]	$130 \pm 5$	–	$130 \pm 6$	–	$150 \pm 4$	–	$159 \pm 6$	77
$q^{\text{[b]}}$	1	0	1	0	1	0	1	1
$\Delta H_M^\ddagger$ [ $\text{kJ mol}^{-1}$ ]	$36.5 \pm 0.6$	–	$21.0 \pm 0.4$	–	$20.4 \pm 0.5$	–	$13.1 \pm 0.6$	49.8
$A/\hbar$ [ $10^6\text{rad s}^{-1}$ ]	$-3.7 \pm 0.1$	–	–3.5	–	–3.6	–	–4.1	–3.8
$q^{\text{[b]}}$	2	2	2	2	2	2	2	–
$r'$ [ $\text{\AA}$ ]	$3.5 \pm 0.1$	$3.5 \pm 0.1$	$3.5 \pm 0.2$	$3.5 \pm 0.1$	$3.8 \pm 0.3$	$3.4 \pm 0.1$	$3.4 \pm 0.2$	–

[a] For the parameters  $r$ ,  $a$ ,  $^{298}D$ ,  $^{310}D$ , and  $E_R$  the values of 3.0, 4.0  $\text{\AA}$ ,  $2.24 \times 10^{-5}$ ,  $3.10 \times 10^{-5} \text{cm}^2\text{s}^{-1}$ , and  $18 \text{kJ mol}^{-1}$ , respectively, were used. [b] Fixed in the fitting procedure. [c] Taken from ref. [23].

enters as a scaling factor in the numerator of Equation (4) and in the corresponding equation for the  $R_2$   $^{17}\text{O}$  data. In the data analysis we have assumed that the  $q$  value obtained from luminescence lifetimes of the  $\text{Tb}^{3+}$  derivative ( $q=0.9$ ) corresponds to the presence of one bound water molecule.

The reduced transverse relaxation rates,  $R_{2r}$ , increase with decreasing temperature, following the behavior of complexes characterized by a fast water exchange rate of the inner-sphere water molecule. In fact, whereas the electronic relaxation parameters ( $\Delta^2$  and  $\tau_V$ ) and the hyperfine coupling constant  $A/\hbar$  assume values rather typical of DOTA-like  $\text{Gd}^{3+}$  complexes, the rate of water exchange is definitely high (Table 2). This may be caused by strong steric interactions between the substituent of the DO3A unit and the coordinated water molecule that decrease the activation enthalpy of the exchange process (low  $\Delta H_M^\ddagger$ ) and thus the mean residence lifetime ( $\tau_M = 14 \text{ns}$  at 298 K). A strictly similar behavior has been recently reported for a  $\text{Gd}$ -DOTA derivative bearing a propionamide arm.<sup>[17]</sup>

As noted above, in the best-fit analysis of the NMRD profiles we need to consider three contributions: inner-sphere (IS), second-sphere (SS), and outer-sphere (OS). We fixed  $q$  (IS),  $r$  (IS; 3.0  $\text{\AA}$ ),  $a$  (OS; 4.0  $\text{\AA}$ ),  $^{298}D$  (OS;  $2.24 \times 10^{-5} \text{cm}^2\text{s}^{-1}$ ),  $^{298}\tau_M$  (IS),  $\Delta^2$  (IS, SS, OS) and  $^{298}\tau_V$  (IS, SS, OS). For the latter three parameters, we utilized the values obtained from  $^{17}\text{O}$  NMR spectroscopic data.

We considered three adjustable parameters  $\tau_R$  (IS; in the range 60–180 ps),  $\tau_{R'}$  (SS; in the range 30–90 ps) and  $q'/r'^6$  (SS). A satisfactory fit was obtained by considering the contribution of two equivalent SS water molecules located at a distance of 3.5  $\text{\AA}$  from the metal ion (Table 2). It is worth emphasizing the fact that this analysis is not entirely rigorous and provides only an estimate of the magnitude of the contribution of SS solvent molecules to the overall relaxivity of the complexes. Clearly, the number of water molecules H-bonded at different distances from the metal center and thus with different lifetimes altogether contribute to the overall SS relaxivity. Recorded at 20 MHz, this contribution represents about 25% of the global relaxivity. It is possible to obtain an estimate of the reliability and consistency of these results by comparing the value of  $\tau_R$  calculated with that of several other monoaqua complexes of similar size. At 20 MHz, the value of  $\tau_R$  presents a good linear correla-

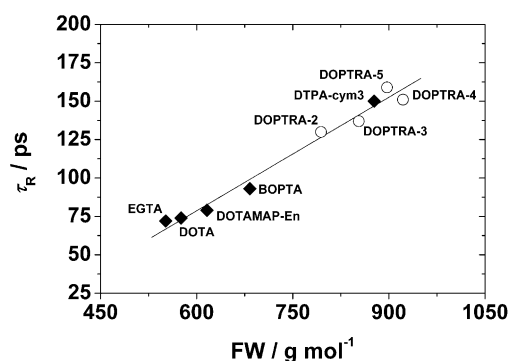


Figure 6. Rotational correlation time,  $\tau_R$ , versus molecular weight for selected  $\text{Gd}^{3+}$  complexes with  $q=1$  (filled symbols;  $R=0.989$  for the straight line) and for the DOPTRA complexes discussed in the present work (open symbols). Data for EGTA (1,1,10,10-tetrakis(carboxymethyl)-1,10-diaza-4,7-dioxadecane), DOTA (1,4,7,10-tetrakis(carboxymethyl)-1,4,7,10-tetraazacyclododecane), DOTAMAP-En (1-(2-(aminoethyl)aminocarbonyl)-ethyl)-4,7,10-tris(carboxymethyl)-1,4,7,10-tetraazacyclododecane) and DTPA(cym)<sub>3</sub> (diethylenetriamine(cyclohexylmethyl)pentacetic acid) are taken from references [18, 16, 17 and 19], respectively.

tion with the molecular mass of small gadolinium complexes, as shown in Figure 6.

The data calculated for  $\text{Gd}$ -DOPTRA-2 follows the expected trend very well, confirming that the calculated parameters represent a good description of the relaxometric properties of the complex.

We followed a similar approach for analyzing the relaxometric data for the complexes  $\text{Gd}$ -DOPTRA-(3–5) in the presence of an excess of  $\text{Ca}^{2+}$ . In the analysis of the data, we have made the choice to approximate the values of  $q$  obtained from the luminescence lifetimes measurements with integers. This is because, given the error associated with this type of measurement, the difference between the calculated non-integer values and those approximated integers seems definitely negligible. The other possible explanation is the presence of equilibrium between a largely prevalent species and another species that differ in their hydration state. However, the use of non-integer  $q$  values of Table 1 in the relaxometric data analysis, as often found in the literature, only marginally changes the results of the fit. We first analyzed the  $^{17}\text{O}$  NMR  $R_2$  and chemical shift profiles versus temperature and then used the values of the parameters ob-

tained to fit the NMRD curves. In the absence of  $\text{Ca}^{2+}$ , only the NMRD profiles have been analyzed.

**Gd-DOPTRA-(3–5):** The  $^1\text{H}$   $1/T_1$  NMRD profiles were recorded at both 25 and 37°C in absence of  $\text{Ca}^{2+}$  (Figure 7, lower curves). At 20 MHz and 298 K, the  $r_1$  values are in the range 4.2–4.6  $\text{mM}^{-1}\text{s}^{-1}$ , about 50% lower than the value for Gd-DOPTRA-2. This result is clearly a consequence of

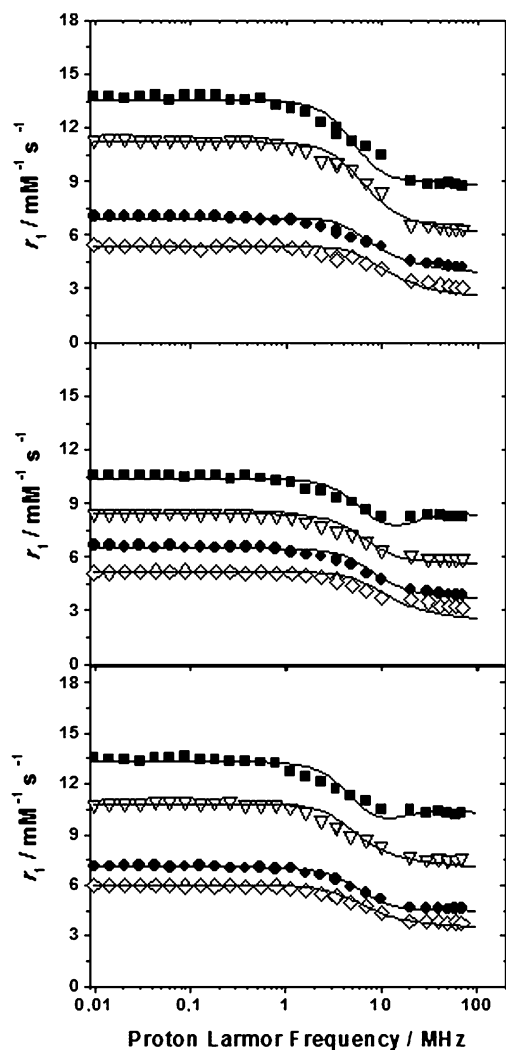


Figure 7.  $^1\text{H}$  NMRD profiles for the Gd-DOPTRA-(3–5), from top to bottom) complexes at 25 (filled symbols) and 37°C (open symbols), before (lower curves) and after (upper curves) the addition of 3 equiv of  $\text{Ca}^{2+}$ . The curves through the experimental data are calculated with the parameters reported in Table 2.

the lower hydration number that indicates the presence (or a large predominance) in solution of the species without a coordinated water molecule. The  $q=0$  complex could be the consequence of the intramolecular coordination of two carboxylates or attributed to the coordination of only one carboxylate group of the pendant arm, which introduces a strong steric hindrance such as to prevent the access of water molecules. In the first case, the complex has a 9-coor-

dinate ground state, whereas in the second it is 8-coordinated. Both situations might occur depending on the length and flexibility of the pendant arm. On the other hand, the relaxivity of the complexes is significantly larger than the values typically reported for  $q=0$  complexes. Clearly, the absence of a coordinated water molecule is compensated by the presence of a number of water molecules hydrogen-bonded to the polar groups of the ligand, hence at a distance sufficiently short from the  $\text{Gd}^{3+}$  to contribute to the observed  $r_1$  values.<sup>[22]</sup> The least-square best-fit procedure was carried out by considering both outer- and second-sphere contributions (SS) to relaxivity. The estimated SS components provide a comparable contribution to  $r_1$  for the three complexes, since the small differences in the calculated parameters (Table 2) cannot be considered significant in light of the approximations inherent in the data analysis. Moreover, this SS contribution is rather comparable to that estimated for Gd-DOPTRA-2.

The  $^1\text{H}$   $1/T_1$  NMRD profiles of the complexes in the presence of three equivalents of  $\text{Ca}^{2+}$  are shown in Figure 7 (upper curves). The temperature dependence of the  $^{17}\text{O}$  NMR  $R_2$  and chemical shift data are shown in Figure 8.

In general, we observe a large relaxivity enhancement when an excess of  $\text{Ca}^{2+}$  is added to the solutions of Gd-DOPTRA-(3–5). At 20 MHz and 298 K,  $r_1$  shows a two-fold increase, from about 4.2–4.6  $\text{mM}^{-1}\text{s}^{-1}$  to about 8.3–10.5  $\text{mM}^{-1}\text{s}^{-1}$ . The large relaxivity values are clearly the result of the occurrence of the IS contribution arising from the presence of a coordinated water molecule ( $q=1$ ). The NMRD profiles not only present a larger amplitude over the entire range of proton Larmor frequencies, but also show the incipient formation of a very broad hump at high fields that is often associated with rotational correlation times of the order of 0.1 ns.<sup>[13b]</sup> In fact, the  $\tau_R$  values are slightly longer than for Gd-DOPTRA-2 and follow the linear relation with the molecular mass of the complexes quite well (Figure 6). In fact, calcium binding not only promotes the formation of highly hydrated species in solution but also tends to restrict the rotational flexibility of the pendant arm, as indicated by the large  $\tau_R$  values.

The parameters associated with the electronic relaxation,  $\Delta^2$  and  $\tau_v$ , have values quite similar to those reported for related DO3A-derivatives and do not vary significantly upon  $\text{Ca}^{2+}$  binding. This supports the hypothesis that the coordination cage around the metal ion remains essentially unchanged. The SS relaxivity provides a smaller relative contribution to the overall relaxivity, although its value remains virtually constant compared with the value in the absence of  $\text{Ca}^{2+}$ . The distance of proton of the second-sphere water from  $\text{Gd}^{3+}$  is about 3.5 Å and it is quite similar to estimates for related complexes.<sup>[20]</sup>

The relaxivity decreases with temperature at any value of the magnetic field strength and this shows that the water residence lifetime,  $\tau_M$ , does not represent a limiting factor. A relatively fast rate of water exchange is to be expected based on the plausible high steric crowding around the coordinated water molecule in the calcium-bound complex.

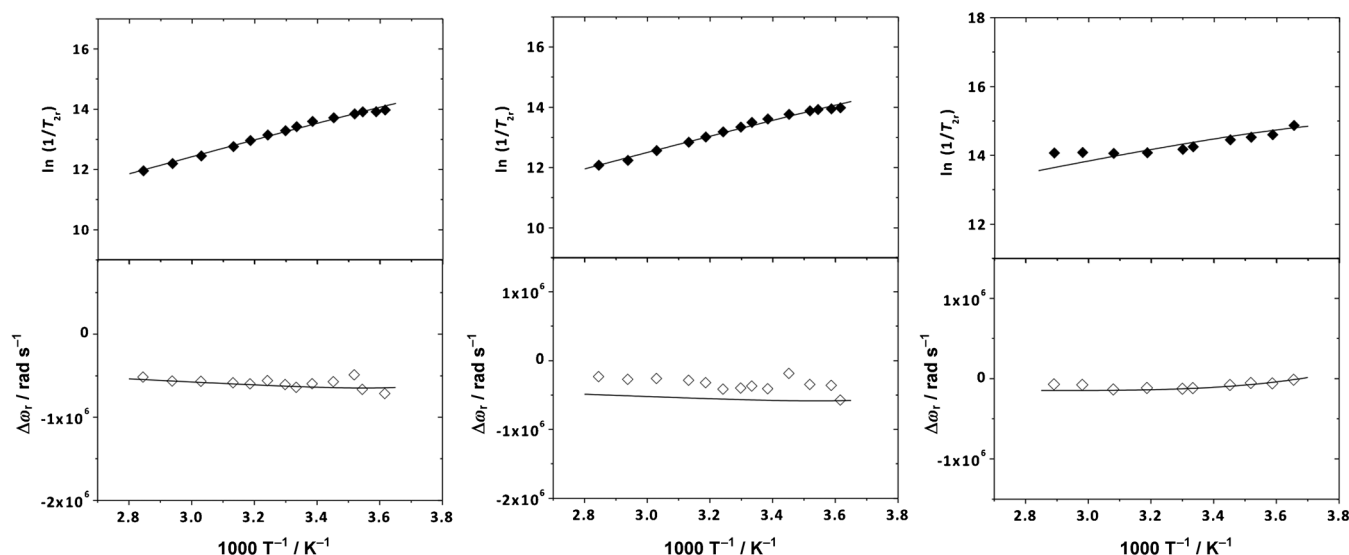


Figure 8. Reduced transverse  $^{17}\text{O}$  relaxation rates (filled symbols) and chemical shifts (open symbols) of aqueous solutions of Gd-DOPTRA-3 (left; 13.0 mm), Gd-DOPTRA-4 (middle; 12.7 mm), and Gd-DOPTRA-5 (right; 8.3 mm) at 11.75 T and neutral pH, after the addition of an excess of  $\text{Ca}^{2+}$ . The solid curves passing through the data are calculated by using the parameters of Table 2.

Changing  $\tau_M$  between 5–100 ns does affect the quality of the fit of the NMRD profiles. Therefore,  $\tau_M$  was more accurately determined by recording the transverse relaxation rates ( $R_{2p}$ ) and shift ( $\Delta\omega$ ) of the  $^{17}\text{O}$  nucleus as a function of temperature (Figure 8). Some parameters were fixed:  $q=1$ , the activation energy of the correlation time for the modulation of the transient zero-field-splitting tensor  $E_V=1.0\text{ kJ mol}^{-1}$  and the activation energy of the rotational correlation time  $E_R=16\text{ kJ mol}^{-1}$ . In addition, for  $\Delta^2$  and  $\tau_V$  we utilized the values derived from the fit of the NMRD profiles. The parameters treated as adjustable were: the mean residence lifetime of the inner sphere water molecule,  $\tau_M$ , its enthalpy of activation  $\Delta H_M^\ddagger$  and the scalar Gd- $^{17}\text{O}_w$  coupling constant,  $A/\hbar$ . An exponential increase in  $R_{2p}$  is observed with decreasing temperature for three complexes, in agreement with a fast exchange regime of the bound water molecule with the surrounding bulk. The  $\tau_M$  values obtained, approximately 10–35 ns, are in the range observed previously for other phosphonate-appended macrocyclic systems.<sup>[21]</sup> The presence of the bulky pendant arm is often associated with a steric crowding around the metal ion that increases the rate of water exchange.<sup>[22]</sup> Accordingly, also the values of the enthalpy of activation,  $\Delta H_M^\ddagger$ , are also small and rather similar to each other. Merbach et al. have reported analogous low values of the activation enthalpy for fast-exchanging Gd-chelates.<sup>[23]</sup> The hyperfine coupling constants (Gd- $^{17}\text{O}$ ) fall in a narrow range of values that are quite typical for Gd $^{3+}$  complexes.<sup>[6,16]</sup> The reduced chemical shifts ( $\Delta\omega_r$ ) are somewhat smaller than for other  $q=1$  Gd-chelates. Smaller values of chemical shifts have been measured in the case of complexes with a significant

second-sphere contribution. The experimental data for Gd-DOPTRA-5 are not of good quality, particularly at high temperatures. This could be due to the limited concentration of the solution (8.3 mm) that limits the accuracy of the calculated paramagnetic contribution. Also, we cannot exclude the change in the hydration state at higher temperatures or a change in population of species with different hydration number.

**Dissociation constant with  $\text{Ca}^{2+}$ :** In the extracellular space of the brain, the  $\text{Ca}^{2+}$  concentration at resting state is 1.2 mM, which decreases up to 30% during normal neural activity. To sense the  $\text{Ca}^{2+}$  concentration fluctuations in the mM range, a smart CA should have a dissociation constant satisfying the condition:  $0.1 \cdot K_d < [\text{Ca}^{2+}] < 10 \cdot K_d$ . To evaluate the dissociation constants of the CAs to  $\text{Ca}^{2+}$  the paramagnetic relaxation enhancement (PRE) method was used.<sup>[7b]</sup> The relaxivity data obtained were fitted to Equation (6).

$$r_{\text{obs}} = \frac{\left\langle r_f[\text{CA}]_f + (r_b - r_a) \left\{ n[\text{CA}]_f + \text{Ca}^{2+} + K_d - \sqrt{\frac{(-n[\text{CA}]_f + [\text{Ca}^{2+}] + K_d)^2 - 4n[\text{CA}]_f[\text{Ca}^{2+}]}{2n}} \right\} \right\rangle}{\text{CA}} \quad (6)$$

in which  $r_{1,\text{obs}}$  is the observed relaxivity,  $r_f$  is the relaxivity of free CA,  $r_b$  is the relaxivity of bound (to  $\text{Ca}^{2+}$ ) CA,  $n$  is the number of  $\text{Ca}^{2+}$  binding sites on CA, and  $K_d$  is the equilibrium dissociation constant. The fitting was done using  $K_d$ ,  $r_f$ , and  $r_b$  as variable parameters and  $n$  was fixed to 1. The dissociation constants obtained are tabulated in Table 3 and the fitting is shown in Figure 9. The other parameters ( $r_f$ ,  $r_b$ ) obtained in the fitting are tabulated in the Supporting Infor-

Table 3. Dissociation constants obtained by fitting the relaxivity data in Equation (3).

CAs	$K_d$ [mM]
Gd-DOPTRA-3	$0.2 \pm 0.01$
Gd-DOPTRA-4	$1.1 \pm 0.1$
Gd-DOPTRA-5	$0.1 \pm 0.01$

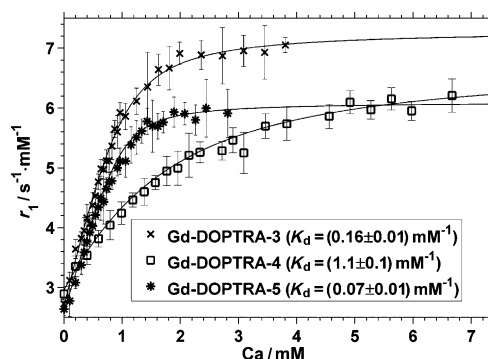
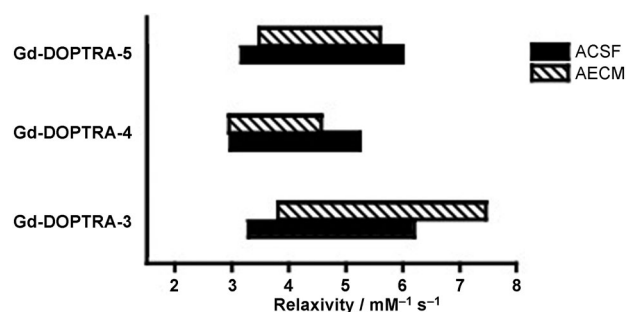


Figure 9. The determination of the dissociation constant by using the paramagnetic relaxation enhancement method.

mation. Data shows that the dissociation constant of the Gd-DOPTRA series are in the desired range for sensing extracellular  $\text{Ca}^{2+}$  concentration changes.

**Selectivity study in ACSF and AECM:** One of the crucial steps for the successful application of any contrast agent is the ability to retain their excellent in vitro response (e.g.,  $\text{Ca}^{2+}$  responsive) in in vivo conditions. To evaluate this ability, it is important to check their selectivity in the complex physiological medium. We selected two different solutions mimicking the in vivo conditions in the brain: an artificial cerebro spinal fluid (ACSF), and an artificial extracellular matrix (AECM). CSF is the fluid that occupies the subarachnoid space and ventricular system around and inside the brain. The extracellular space of the brain freely communicates with the CSF compartment and therefore the compositions of two fluids are similar. The prepared ACSF contains all the major anions and cations present in CSF ( $\text{Na}^+$ ,  $\text{K}^+$ ,  $\text{Mg}^{2+}$ ,  $\text{Cl}^-$ ,  $\text{HCO}_3^-$ ; refer to the Supporting Information for the chart). ECM on the other hand is a lattice of proteins, polysaccharide, and compounds attached to the plasma membrane (refer to the Supporting Information for a chart). ECM materials are mostly present in intercellular spaces between neurons and glia.<sup>[24]</sup> In addition to all the major proteins, AECM also contains all the main anions and cations present in actual ECM. In ACSF the amount of relaxivity change for Gd-DOPTRA-(3–5) was observed to be  $\approx 90$ , 75, and 85%, whereas in AECM it was observed to be  $\approx 95$ , 50, and 61%, respectively (Figure 10). These significant improvements, if observed in vivo, might be sufficient for the visualization of  $\text{Ca}^{2+}$  concentration changes by MRI.

Figure 10.  $\text{Ca}^{2+}$  dependent relaxivity responses of Gd-DOPTRA-(3–5) in physiological fluids (pH 7.4) at 400 MHz. The horizontal bar represents the change in relaxivity upon  $\text{Ca}^{2+}$  addition to CAs solution in ACSF or AECM.

## Conclusion

A new set of APTRA-based contrast agents (Gd-DOPTRA-(3–5)), designed to sense  $\text{Ca}^{2+}$  concentration changes in the extracellular matrix of the brain following neural activity, are reported. The introduction of a single carbon unit in the linker connecting the aromatic unit to Gd-DO3A provided the desired structural stability. Besides stability, Gd-DOPTRA-(3–5) have exhibited excellent longitudinal relaxivity enhancement in the presence of  $\text{Ca}^{2+}$  from simple buffer solution to complex biological fluids such as ACSF and AECM. The dissociation constant of the CAs to  $\text{Ca}^{2+}$  ranged from 0.1 to 1.4 mM, which is the desired range to bind  $\text{Ca}^{2+}$  in the extracellular matrix of the brain where its concentration ranges from  $0.8 \mu\text{M}$  to  $1.2 \text{mM}$ . The origin of the relaxivity enhancement was studied in great detail by luminescence lifetime measurement, NMRD, and  $^{17}\text{O}$  NMR spectroscopy. The results of these studies confirmed that the large relaxivity enhancement observed upon  $\text{Ca}^{2+}$  addition is due to the increase of the hydration state of the complexes together with the slowing down of the molecular rotation and the retention of a significant contribution of the water molecules of the second sphere of hydration. The improvement in the  $\text{Ca}^{2+}$  specific relaxivity response of the CAs and the desired dissociation constants makes Gd-DOPTRA-(3–5) promising candidates for in vivo evaluations, which are under way in our laboratory.

## Experimental Section

**General:** All chemicals were purchased of the purest grade from commercial sources and were used without further purification. The anhydrous THF was obtained by freshly distilling it from sodium and benzophenone. Unless otherwise mentioned all reactions were carried out under nitrogen atmosphere and the flasks were dried with heat gun under vacuum. The distilled water was used for the reaction work up and MilliQ water was used throughout after the last deprotection steps.  $^1\text{H}$  and  $^{13}\text{C}$  NMR spectroscopic analysis of all the ligands and the intermediates were performed on a Bruker 400, 300, or 250 MHz spectrometer.  $^1\text{H}$  and  $^{13}\text{C}$  NMR spectra were performed in deuterated solvents and chemical shifts were assigned by comparison with the residual proton and carbon resonance of the solvents and tetramethylsilane as the internal

reference ( $\delta=0$  ppm). Data are reported as follows: chemical shift (multiplicity: s=singlet, d=doublet, t=triplet, dd=double of doublet, brs=broad singlet, J=coupling constant (Hz), integration, peak assignment in italic form). ESI low resolution mass spectra (ESI-MS) were recorded on SL 1100 system (Agilent, Germany) with ion trap detection in positive and negative mode. ESI high resolution mass spectras (ESI-HRMS) were performed on a Bruker Daltonics Apex II FT-ICR-MS (Bruker, Germany). Inductively coupled plasma optical emissions spectrometry (ICP-OES) was performed on a Jobin Yvon Ultima 2 ICP-OES at the Department of Chemistry, Durham University, UK.

Column chromatography was performed by using silica gel 60 (70–230 mesh) purchased from Merck as stationery phase. Analytical thin layer chromatography (TLC) was performed on aluminum sheet silica gel plates with 0.2 mm thick silica gel 60 F254 (E. Merck, Germany) using different solvent system as mobile phase. The compounds were visualized by UV254 light and the chromatographic plates were developed in Iodine chamber or aqueous solution of molybdophosphorous acid. The molybdate solution as prepared by ammonium molybdate  $\text{Mo}_7\text{O}_{24}(\text{NH}_4)_6 \cdot 4\text{H}_2\text{O}$  (20 g) and  $\text{Ce}(\text{SO}_4)_2 \cdot 4\text{H}_2\text{O}$  (0.4 g) were dissolved in of 10%  $\text{H}_2\text{SO}_4$  (400 mL).

RP-HPLC was performed at room temperature on a Varian PrepStar Instrument, Australia, equipped with PrepStar SD-1 pump heads. UV absorbance was measured by using ProStar 335 photodiode array detector at 214 and 254 nm. All solvents used were of HPLC grade and were bought from Merck-VWR and used without further purifications. Analytical HPLC was performed in a stainless steel Chromsep (length 250 mm, internal diameter 4.6 mm, outside diameter 3/8 inch and particle size 8  $\mu\text{m}$ ) C18 column. For semi-preparative HPLC stainless steel Polaris (21.2  $\times$  250 mm, 5  $\mu\text{m}$ , 100  $\text{\AA}$ ), Varian column was used with flow rate of 15  $\text{mL min}^{-1}$ . A gradient method was used starting with 95% solvent A ( $\text{H}_2\text{O}$ , 0.1%  $\text{HCOOH}$ ) and 5% solvent B (acetonitrile, 0.1%  $\text{HCOOH}$ ) to 70% solvent B in 10 min and then to 100% in next 8 min running isocratic for 12 min after that and then back to 5% solvent B in next 2 min.

The  $\text{Tb}^{3+}$  luminescence lifetime measurements were performed using a neodymium-doped yttrium aluminum garnet (Nd:YAG) Continuum Powerlite 8010 laser (354 nm, third harmonic) as the excitation source. Emission was collected at a right angle to the excitation beam, and signals arising from the  $^5\text{D}_4 \rightarrow ^7\text{F}_3$   $\text{Tb}^{3+}$  transition (545 nm) were selected by a Spectral Products CM 110 1/8 meter monochromator. The signal was monitored using a Hamamatsu R928 photomultiplier coupled to a 500 MHz band pass digital oscilloscope (Tektronix TDS 754D). For each flash, the experimental decay was recorded with a resolution of 50000 points. To minimize experimental contribution, signals from >1000 flashes were collected and averaged. Luminescence decay curves were analyzed with Origin 7.0 software. The experimental decay curves were fitted to a single exponential model using the Chi-squared criteria to discriminate the best exponential fit.

**NMRD and  $^{17}\text{O}$  NMR spectroscopic measurements:** The exact concentrations of gadolinium were determined by measurement of bulk magnetic susceptibility shifts of a  $t\text{BuOH}$  signal on a Bruker Avance III spectrometer (11.7 T). The proton  $1/T_1$  NMRD profiles were measured on a fast field-cycling Stellar SmartTracer relaxometer over a continuum of magnetic field strengths from 0.00024 to 0.25 T (corresponding to 0.01–10 MHz proton Larmor frequencies). The relaxometer operates under computer control with an absolute uncertainty in  $1/T_1$  of  $\pm 1\%$ . Additional data points in the range 15–70 MHz were obtained on a Bruker WP80 NMR electromagnet adapted to variable-field measurements (15–80 MHz proton Larmor frequency) Stellar Relaxometer. The  $^1\text{H}$   $T_1$  relaxation times were acquired by the standard inversion recovery method with typical  $90^\circ$  pulse width of 3.5  $\mu\text{s}$ , 16 experiments of 4 scans. The reproducibility of the  $T_1$  data was  $\pm 5\%$ . The temperature was controlled with a Stellar VTC-91 airflow heater equipped with a calibrated copper-constantan thermocouple (uncertainty of  $\pm 0.1^\circ\text{C}$ ).

Variable-temperature  $^{17}\text{O}$  NMR measurements were recorded on a Bruker Avance III (11.7 T) spectrometer equipped with a 5 mm probe and standard temperature control units. Aqueous solutions of the complex containing 2.0% of the  $^{17}\text{O}$  isotope (Cambridge Isotope) were used.

The observed transverse relaxation rates were calculated from the signal width at half-height.

A  $\text{Ca}^{2+}$ -free ACSF solution was prepared by making a 100 mL standard solution of 4-(2-hydroxyethyl)-1-piperazineethanesulfonic acid (HEPES) buffer (1.668 g), NaCl (0.723 g), KCl (0.0216 g),  $\text{MgCl}_2 \cdot 6\text{H}_2\text{O}$  (0.01423 g) and  $\text{NaHCO}_3$  (0.1957 g). The pH of the finally obtained solution was adjusted at pH 7.4 by the addition of solid KOH. Stock solution of AECM was prepared afresh by mixing 5 mL of Dulbecco's Modified Eagle Medium (DMEM) liquid (high glucose) (Invitrogen, Catalog Number: 21068028), 5 mL of F-12 Nutrient Mixture (Ham) (Invitrogen, Catalog Number: 21765029) and 100  $\mu\text{L}$  of N-2 Supplement liquid (Invitrogen, Catalog Number: 17502048). The exact compositions are listed in the Supporting Information.

The  $T_1$  measurements were performed on a 400 MHz Bruker advance spectrometer using the system software Topspin for data acquisition and  $T_1$  evaluation. An inversion-recovery measurement was used with 32 logarithmic inversion time steps between 50  $\mu\text{s}$  and 3 s. The inversion delay was 6 s and the power for the  $90^\circ$  reference pulse was adjusted for every sample individually.  $T_1$  was calculated by fitting the intensities ( $I$ ) of the spectrum proton peaks into Equation (7):

$$I_{(t_i)} = I_0(1 - 2A \exp(-t_i/T_1)) \quad (7)$$

in which  $I_{(t_i)}$  is the measured proton peak intensity at inversion time  $t_i$ ,  $I_0$  is the proton peak intensity without inversion,  $T_1$  is longitudinal relaxation time and factor  $A$  takes the finite inversion delay in to account. The samples were measured in 40  $\mu\text{L}$  capillary tubes inserted in 5 mm NMR tubes. The relaxation rate of the solvent in absence of a paramagnetic solute ( $R_{1d} = 1/T_{1d}$ ) was determined from the plot of different concentrations of CAs versus  $R_{1\text{obs}}$  (observed relaxation rate,  $1/T_{1\text{obs}}$ ) by linear regression. Gd concentrations ( $[\text{Gd}]$ ) were determined by ICP-OES.

**Synthesis: 3-(Benzyloxy)-2-nitrobenzaldehyde (1):** Borontribromide (3.0 mL, 30.3 mmol) was added dropwise to a solution of 3-methoxy 2-nitro benzaldehyde (2.5 g, 13.8 mmol) in  $\text{CH}_2\text{Cl}_2$  (70 mL) under dry ice. After the addition was complete, the reaction mixture (RM) was stirred at the same temperature for 30 min. MeOH was the slowly added to quench the reaction. The RM was removed from cooling bath and the solvent was evaporated under vacuum. The crude product obtained was mixed with  $\text{K}_2\text{CO}_3$  (4.7 g, 34.5 mmol) and MeCN (60 mL), and heated at  $60^\circ\text{C}$  for 1 h. The contents were then removed from heating and benzyl bromide (2.5 mL, 20.7 mmol) was added. This was heated again at  $60^\circ\text{C}$  for another 2 h. The RM was filtered, washed with  $\text{CH}_2\text{Cl}_2$ , and concentrated under vacuum. The yellow oil obtained was chromatographed and purified in ethyl acetate/hexane (0.2:1) solvent mixture to obtain the product as light-yellow solid (3.0 g, 85%).  $^1\text{H}$  NMR (400 MHz,  $\text{CDCl}_3$ ):  $\delta=4.99$  (s, 2H), 7.09–7.18 (m, 6H), 7.24 (d,  $J=7.63$  Hz, 1H), 7.34 (t,  $J=8.01$  Hz, 1H), 9.69 ppm (s, 1H);  $^{13}\text{C}$  NMR (100 MHz,  $\text{CDCl}_3$ ):  $\delta=70.9$ , 119.7, 122.5, 126.6, 127.5, 128.0, 128.3, 131.2, 134.4, 139.6, 149.5 ppm; ESI-MS:  $m/z$  calcd for  $\text{C}_{14}\text{H}_{11}\text{NO}_4$ : 312.08424 [ $\text{C}_{14}\text{H}_{11}\text{NO}_4 + \text{CH}_3\text{OH} + \text{Na}$ ] $^+$ ; found: 312.08420.

**3-(Benzyloxy)-2-nitrophenylmethanol (2):** Compound **1** (2.0 g, 7.8 mmol) was dissolved in minimum amount of  $\text{CH}_2\text{Cl}_2$  (dry). MeOH (dry, 30 mL) was added and the RM was kept in an ice bath. Sodium borohydride (0.1 g, 2.6 mmol) was added to RM in small portions. After complete addition, the RM was stirred at RT for 2 h. The reaction was quenched by the dropwise addition of saturated  $\text{NaHCO}_3$  solution. The RM was concentrated under vacuum, re-dissolved in  $\text{CH}_2\text{Cl}_2$  (200 mL) and washed with water ( $3 \times 200$  mL). The organic layer was collected, dried under anhydrous  $\text{Na}_2\text{SO}_4$ , and concentrated under vacuum. The crude mixture obtained was flash chromatographed in  $\text{CH}_2\text{Cl}_2$  to obtain the desired product as light-yellow solid (1.9 g, 90%).  $^1\text{H}$  NMR (400 MHz,  $\text{CDCl}_3$ ):  $\delta=4.45$  (s, 2H), 4.99 (s, 2H), 6.84 (d,  $J=8.39$  Hz, 1H), 6.93 (d,  $J=7.88$  Hz, 1H), 7.12–7.27 ppm (m, 6H);  $^{13}\text{C}$  NMR (100 MHz,  $\text{CDCl}_3$ ):  $\delta=60.4$ , 70.6, 113.2, 120.2, 126.6, 127.8, 128.2, 131.7, 133.9, 135.1, 139.9, 149.5 ppm; ESI-MS:  $m/z$  calcd for  $\text{C}_{14}\text{H}_{13}\text{NO}_4$ : 298.04762 [ $\text{C}_{14}\text{H}_{13}\text{NO}_4 + \text{K}$ ] $^+$ , found 298.04770.

**1-(Benzyloxy)-3-(bromomethyl)-2-nitrobenzene (3):**  $\text{PPh}_3$  (3.6 g, 13.8 mmol) was added to a solution of **2** (1.8 g, 6.9 mmol) in  $\text{CH}_2\text{Cl}_2$  (dry,

50 mL) under ice, followed by addition of carbon tetrabromide (4.8 g, 14.5 mmol) in small portions. The RM was stirred for 1 h at RT. The solvent was then removed under vacuum and the crude oil obtained was purified by column chromatography using ethyl acetate/hexane (0.1:1) solvent mixture to obtain the product as yellow oil (1.7 g, 77%). <sup>1</sup>H NMR (400 MHz, CDCl<sub>3</sub>): δ = 4.20 (s, 2H), 4.89 (s, 2H), 6.80 (t, 2H), 7.05–7.19 ppm (m, 6H); <sup>13</sup>C NMR (100 MHz, CDCl<sub>3</sub>): δ = 26.4, 71.2, 114.6, 122.8, 127.1, 128.4, 128.8, 130.8, 131.6, 135.4, 141.1, 150.2 ppm; ESI-MS: *m/z* calcd for C<sub>14</sub>H<sub>12</sub>BrNO<sub>3</sub>: 343.98928 [C<sub>14</sub>H<sub>12</sub>BrNO<sub>3</sub>+Na]<sup>+</sup>; found: 343.98911.

*Tri-tert-butyl 2,2',2''-(10-(3-(benzyloxy)-2-nitrobenzyl)-1,4,7,10-tetraazacyclododecane-1,4,7-triyl)triacetate (4)*: K<sub>2</sub>CO<sub>3</sub> (2.7 g, 19.4 mmol) was added to a solution of *tris-tert-Bu-DO3A* (4.0 g, 7.8 mmol) in DMF (dry, 10 mL), and the resulting mixture was heated for 1 h at 60°C. Compound **3** (3.2 g, 10.1 mmol) was dissolved in DMF (dry, 5 mL) and added slowly to the RM. The resulting mixture was heated at the same temperature overnight. It was then filtered, the solvent evaporated and the residue was re-dissolved in CH<sub>2</sub>Cl<sub>2</sub> (400 mL). The organic layer was washed with water (3 × 300 mL), dried with anhydrous Na<sub>2</sub>SO<sub>4</sub>, and evaporated under vacuum to a yellow oil. This was purified by column chromatography in MeOH/CH<sub>2</sub>Cl<sub>2</sub> (0.02–0.05:1) to obtain a light-yellow oil (2.3 g, 40%). <sup>1</sup>H NMR (300 MHz, CDCl<sub>3</sub>): δ = 1.31–1.46 (m, 27H), 2.02–2.44 (m, 2H), 2.56 (brs, 4H), 2.64–2.95 (m, 10H), 3.00 (brs, 2H), 3.25 (s, 4H), 3.49 (brs, 2H), 5.05–5.17 (m, 2H), 6.82–7.07 (m, 1H), 7.11–7.38 ppm (m, 7H); <sup>13</sup>C NMR (75 MHz, CDCl<sub>3</sub>): δ = 27.7, 27.9, 28.07, 28.12, 50.2, 51.9, 52.3, 53.8, 55.7, 55.8, 56.04, 56.14, 70.9, 82.3, 82.8, 112.8, 113.3, 122.2, 122.6, 126.90, 126.98, 128.0, 128.2, 128.5, 128.6, 135.2, 135.6, 141.7, 143.3, 149.5, 149.6, 172.6, 173.4 ppm; ESI-MS: *m/z* calcd for C<sub>40</sub>H<sub>61</sub>N<sub>5</sub>O<sub>9</sub>: 378.73074 [C<sub>40</sub>H<sub>61</sub>N<sub>5</sub>O<sub>9</sub>+2H]<sup>2+</sup>; found: 378.73094.

*Tri-tert-butyl-2,2',2''-(10-(2-amino-3-hydroxybenzyl)-1,4,7,10-tetraazacyclododecane-1,4,7-triyl)triacetate (5)*: Compound **4** (2.0 g, 2.6 mmol) was dissolved in MeOH (15 mL) and Pd/C (10%, w/w) catalyst was added. The heterogenous mixture was stirred for 6 h under H<sub>2</sub> atmosphere (3 atm) in a Parr apparatus. The RM was filtered and the solvent was evaporated to obtain a yellow oil (1.7 g, 89%). This was used for the next reaction without further purification. <sup>1</sup>H NMR (300 MHz, CDCl<sub>3</sub>): δ = 1.37 (s, 5H), 1.40–1.46 (m, 22H), 2.48–2.63 (m, 2H), 2.63–2.93 (m, 11H), 2.93–3.05 (m, 2H), 3.10 (s, 2H), 3.21–3.29 (m, 2H), 3.33 (s, 2H), 6.40–6.63 (m, 2H), 6.73–6.86 ppm (m, 1H); <sup>13</sup>C NMR (75 MHz, D<sub>2</sub>O): δ = 28.3, 28.4, 48.9, 49.2, 52.1, 52.4, 55.9, 58.9, 82.5, 83.1, 115.9, 119.5, 123.9, 124.2, 133.7, 146.3, 172.8, 173.0 ppm; ESI-MS: calcd for C<sub>33</sub>H<sub>57</sub>N<sub>5</sub>O<sub>7</sub>: 363.43308 [C<sub>33</sub>H<sub>57</sub>N<sub>5</sub>O<sub>7</sub>+H]<sup>+</sup>; found: 636.43364.

*2,2',2''-(10-(2-Amino-3-hydroxybenzyl)-1,4,7,10-tetraazacyclododecane-1,4,7-triyl)triacetic acid (6)*: Compound **5** (1.5 g, 2.3 mmol) was dissolved in minimum amount of CH<sub>2</sub>Cl<sub>2</sub> (ca. 2 mL) followed by addition of TFA (20 mL) to this solution. The RM was stirred overnight at RT and then evaporated under vacuum. The crude oil was re-dissolved in CH<sub>2</sub>Cl<sub>2</sub> (2 × 25 mL) and MeOH (2 × 25 mL) and evaporated until dry. The crude oil was purified by RP-HPLC to obtain the desired product as transparent solid (0.4 g, 36%). <sup>1</sup>H NMR (300 MHz, D<sub>2</sub>O): δ = 2.53–2.84 (m, 5H), 2.84–3.03 (m, 3H), 3.03–3.19 (m, 4H), 3.18–3.45 (m, 8H), 3.45–4.07 (m, 4H), 6.75 (d, 1H), 6.82 (d, 1H), 7.11 ppm (dd, 1H); <sup>13</sup>C NMR (75 MHz, D<sub>2</sub>O): δ = 47.89, 47.97, 49.8, 49.9, 51.37, 51.44, 53.1, 54.5, 55.5, 111.9, 114.8, 116.5, 117.7, 120.6, 124.7, 130.1, 150.7, 169.4, 175.4 ppm; ESI-MS: *m/z* calcd for C<sub>21</sub>H<sub>33</sub>N<sub>5</sub>O<sub>7</sub>: 468.24527 [C<sub>21</sub>H<sub>33</sub>N<sub>5</sub>O<sub>7</sub>+H]<sup>+</sup>; found: 468.24541.

*2,2',2''-(10-(2-(Bis(carboxymethyl)amino)-3-(carboxymethoxy)benzyl)-1,4,7,10-tetraazacyclododecane-1,4,7-triyl)triacetic acid (7)*: A solution of aniline **6** (0.1 g, 4.3 mmol) in water (8.0 mL) was taken in a three-neck round bottom flask equipped with a pH meter and a water condenser. The pH was adjusted to 10 using solid NaOH followed by addition of bromoacetic acid (0.22 g, 1.6 mmol). The reaction mixture was heated to 90°C. The pH was maintained at 10 by occasional addition of solid NaOH. After the pH remained constant, the RM was heated for additional 2 h at pH 11. It was then cooled down to RT and the pH was adjusted to 7 with 1 N HCl. The water was evaporated under vacuum and the obtained residue purified by RP-HPLC to obtain the desired product as transparent solid (0.06 g 44%). <sup>1</sup>H NMR (250 MHz, D<sub>2</sub>O): δ = 2.97–

3.55 (m, 22H), 3.73 (brs, 2H), 3.81–4.03 (m, 4H), 4.68 (s, 2H), 6.89 (d, *J* = 3.66 Hz, 1H), 7.05–7.22 (m, 2H); <sup>13</sup>C NMR (62 MHz, D<sub>2</sub>O): δ = 46.6, 47.2, 47.3, 47.9, 50.9, 51.9, 53.2, 52.3, 63.3, 111.8, 119.6, 126.8, 136.8, 153.7, 171.4, 174.5 ppm; ESI-MS: *m/z* calcd for C<sub>27</sub>H<sub>39</sub>N<sub>5</sub>O<sub>13</sub>: 642.2 [C<sub>27</sub>H<sub>39</sub>N<sub>5</sub>O<sub>13</sub>+H]<sup>+</sup>; found: 642.3.

*3-(3-(Benzyloxy)-2-nitrobenzyloxy)propan-1-ol (8)*: In an oven dried flask, sodium hydride (60% emulsion in oil; 0.8 g, 15.4 mmol) was dispersed in THF (dry, 2.0 mL) under N<sub>2</sub>. After 10 min of stirring under ice, compound **2** (2.0 g, 7.7 mmol) dissolved in THF (dry, 5 mL) was added slowly. The RM was stirred at the same temperature for 20 min. Bromopropanol (1.7 mL, 19.3 mmol) was added dropwise and stirring was continued at RT overnight. The excess NaH was quenched by dropwise addition of water and the obtained mixture was extracted with CHCl<sub>3</sub>. The organic layer was collected, dried with anhydrous Na<sub>2</sub>SO<sub>4</sub> and concentrated under vacuum to obtain yellow oil. The crude oil obtained was purified by column chromatography using ethyl acetate/hexane as the solvent mixture. The unused reactant (compound **39**) was recovered (0.5 g, 1.9 mmol) at (0.2:1), whereas the product was obtained at (0.3:1) as yellow solid (1.5 g, 83%). <sup>1</sup>H NMR (300 MHz, CDCl<sub>3</sub>): δ = 1.53–1.64 (m, 2H), 3.35 (t, *J* = 5.85 Hz, 2H), 3.48 (t, *J* = 5.85 Hz, 2H), 4.29 (s, 2H), 4.90 (s, 2H), 6.78 (t, *J* = 7.38 Hz, 2H), 7.02–7.18 ppm (m, 6H); <sup>13</sup>C NMR (62 MHz, CDCl<sub>3</sub>): δ = 31.9, 60.3, 68.7, 68.9, 70.9, 113.7, 120.6, 126.8, 128.0, 128.5, 130.9, 131.7, 135.4, 140.5, 149.8 ppm; ESI-HRMS: *m/z* calcd for C<sub>17</sub>H<sub>19</sub>NO<sub>5</sub>: 340.11554 [C<sub>17</sub>H<sub>19</sub>NO<sub>5</sub>+Na]<sup>+</sup>; found: 340.11542.

*1-(Benzyloxy)-3-((3-bromopropoxy)methyl)-2-nitrobenzene (9)*: Compound **9** was synthesized from compound **8** (3.5 g, 10.9 mmol), in a synthesis similar to that of compound **3** from **2**. The product was eluted with ethyl acetate/hexane (0.2:1) solvent mixture and concentrated under vacuum to a light-yellow oil (3.6 g, 82%). <sup>1</sup>H NMR (300 MHz, CDCl<sub>3</sub>): δ = 2.07–2.18 (m, 2H), 3.51 (t, *J* = 6.49 Hz, 1H), 3.58 (t, *J* = 5.72 Hz, 1H), 4.56 (s, 2H), 5.18 (s, 2H), 7.04 (dd, *J* = 10.55, 8.27 Hz, 2H), 7.29–7.50 ppm (m, 6H); <sup>13</sup>C NMR (75 MHz, CDCl<sub>3</sub>): δ = 30.7, 32.9, 68.7, 69.0, 71.4, 114.1, 121.0, 127.3, 128.5, 128.9, 131.3, 132.2, 135.8, 150.3 ppm; ESI-MS: *m/z* calcd for C<sub>17</sub>H<sub>18</sub>BrNO<sub>4</sub>: 402.03114 [C<sub>17</sub>H<sub>18</sub>BrNO<sub>4</sub>+Na]<sup>+</sup>; found: 402.03124.

*Tri-tert-butyl 2,2',2''-(10-(3-(3-(benzyloxy)-2-nitrobenzyloxy)propyl)-1,4,7,10-tetraazacyclododecane-1,4,7-triyl)triacetate (10)*: Compound **10** was synthesized from compound **9** (3.0 g, 7.9 mmol) in a similar synthesis to that of compound **4** from compound **3**. The product was obtained as yellow solid (3.0 g, 50%) by eluting with MeOH/CH<sub>2</sub>Cl<sub>2</sub> (0.05:1) solvent mixture. <sup>1</sup>H NMR (300 MHz, CDCl<sub>3</sub>): δ = 1.41 (s, 27H), 1.61–1.76 (m, 1H), 1.91–2.10 (m, 1H), 2.19–2.55 (m, 4H), 2.77 (brs, 6H), 2.86 (s, 1H), 2.94 (s, 1H), 2.97–3.22 (m, 5H), 3.31 (s, 3H), 3.41 (s, 4H), 3.54 (t, *J* = 5.21 Hz, 2H), 4.51 (d, *J* = 20.85 Hz, 2H), 5.16 (s, 2H), 6.97 (t, *J* = 7.12 Hz, 1H), 7.05 (dd, *J* = 8.39, 2.80 Hz, 1H), 7.29–7.42 ppm (m, 6H); <sup>13</sup>C NMR (100 MHz, CDCl<sub>3</sub>): δ = 28.2, 28.3, 28.5, 48.2, 50.5, 50.8, 52.3, 53.3, 53.5, 55.7, 56.1, 57.2, 67.9, 69.2, 69.8, 70.0, 71.48, 71.5, 82.14, 82.8, 83.2, 114.3, 114.7, 121.0, 121.7, 127.4, 128.6, 129.0, 135.9, 141.1, 150.4, 150.5, 170.4, 170.7, 172.9 ppm; ESI-MS: *m/z* calcd for C<sub>43</sub>H<sub>67</sub>N<sub>5</sub>O<sub>10</sub>: 407.75167 [C<sub>43</sub>H<sub>67</sub>N<sub>5</sub>O<sub>10</sub>/2+H]<sup>+</sup>; found: 407.75186.

*Tri-tert-butyl-2,2',2''-(10-(3-(2-amino-3-hydroxybenzyloxy)propyl)-1,4,7,10-tetraazacyclododecane-1,4,7-triyl)triacetate (11)*: Compound **11** (2.0 g, 95%) was obtained from compound **10** (2.5 g, 3 mmol) in a similar synthesis to that of compound **5** from compound **4**. <sup>1</sup>H NMR (300 MHz, CDCl<sub>3</sub>): δ = 1.38 (s, 9H), 1.42 (s, 18H), 1.53–1.67 (m, 2H), 2.13–2.52 (m, 12H), 2.53–2.86 (m, 6H), 3.05 (s, 6H), 3.37 (t, 2H), 4.43 (s, 2H), 6.44–6.55 (m, 2H), 7.10 ppm (s, 1H); <sup>13</sup>C NMR (75 MHz, CDCl<sub>3</sub>): δ = 27.7, 27.8, 49.9, 50.1, 51.4, 55.6, 56.3, 67.9, 71.9, 82.3, 82.7, 115.6, 117.4, 120.8, 122.8, 134.5, 144.5, 172.4, 173.3 ppm; ESI-HRMS: *m/z* calcd for C<sub>36</sub>H<sub>63</sub>N<sub>5</sub>O<sub>8</sub>: 694.47494 [C<sub>36</sub>H<sub>63</sub>N<sub>5</sub>O<sub>8</sub>+H]<sup>+</sup>; found: 694.47654.

*2,2',2''-(10-(3-(2-Amino-3-hydroxybenzyloxy)propyl)-1,4,7,10-tetraazacyclododecane-1,4,7-triyl)triacetic acid (12)*: Compound **12** (0.8, 53%) was obtained from compound **11** (2 g, 2.9 mmol) similarly to the synthesis of compound **6** from compound **5**. <sup>1</sup>H NMR (250 MHz, D<sub>2</sub>O): δ = 1.82 (brs, 2H), 3.08 (s, 18H), 3.28–3.51 (m, 6H), 3.58 (brs, 2H), 4.47 (s, 2H), 6.74 (brs, 1H), 6.85 (brs, 1H), 6.98 ppm (brs, 1H); <sup>13</sup>C NMR (62 MHz, D<sub>2</sub>O): δ = 24.1, 49.4, 49.7, 50.9, 51.5, 55.1, 55.8, 67.9, 70.0, 115.2, 116.5, 118.2,

121.6, 121.9, 127.2, 130.2, 149.0, 162.7, 163.1 ppm; ESI-MS: *m/z* calcd for C<sub>24</sub>H<sub>39</sub>N<sub>4</sub>O<sub>8</sub>: 526.28714 [C<sub>24</sub>H<sub>39</sub>N<sub>4</sub>O<sub>8</sub>+H]<sup>+</sup>; found: 526.28604.

**2,2',2''-(10-(3-(2-(Bis(carboxymethyl)amino)-3-(carboxymethoxy)benzyloxy)propyl)-1,4,7,10-tetraazacyclododecane-1,4,7-triyl)triacetic acid (13)**: The ligand **13** (0.058 g, 44%) was obtained from compound **12** (0.1 g, 0.19 mmol) in a similar synthesis to that of ligand **7** from compound **6**. <sup>1</sup>H NMR (250 MHz, D<sub>2</sub>O): δ = 1.89 (brs, 2H), 2.80–2.91 (m, 4H), 2.91–3.02 (m, 4H), 3.10–3.22 (m, 6H), 3.26 (brs, 4H), 3.31 (brs, 2H), 3.36–3.47 (m, 2H), 3.48–3.57 (m, 2H), 3.70 (s, 2H), 4.01 (brs, 4H), 4.63 (s, 2H), 4.65 (s, 2H), 6.81 (t, *J* = 8.01 Hz, 2H), 7.13 ppm (t, *J* = 8.01 Hz, 1H); <sup>13</sup>C NMR (62 MHz, D<sub>2</sub>O): δ = 25.3, 50.86, 50.97, 52.2, 54.3, 55.9, 58.7, 62.0, 68.1, 70.4, 73.1, 116.3, 125.1, 132.1, 135.6, 137.3, 155.9, 172.45, 175.8, 176.7, 176.8 ppm; ESI-MS: *m/z* calcd for C<sub>30</sub>H<sub>45</sub>N<sub>5</sub>O<sub>14</sub>: 700.3 [C<sub>30</sub>H<sub>45</sub>N<sub>5</sub>O<sub>14</sub>+H]<sup>+</sup>; found: 700.2.

**2-Bromo-1-morpholinoethanone (19)**: Morpholine (dry) (3.5 mL, 40 mmol) was dissolved in diethyl ether (dry, 70 mL) and triethylamine (11.0 mL, 80 mmol). After 1 h, the RM was cooled down to 0°C and bromoacetyl bromide (5.2 mL, 60 mmol) was added dropwise. After complete addition, the RM was stirred for another 2 h at 0°C. The salts formed were filtered off and the residue was washed with diethyl ether and concentrated under vacuum. The diethyl ether layer was collected, dried under saturated Na<sub>2</sub>SO<sub>4</sub> and evaporated to brown oil. This was purified by column chromatography using ethyl acetate/CH<sub>2</sub>Cl<sub>2</sub> (0.2:1) as the solvent mixture to obtain the pure product (4.0 g, 48%) as oil. <sup>1</sup>H NMR (300 MHz, CDCl<sub>3</sub>): δ = 3.50 (t, *J* = 5.10, 4.53 Hz, 2H), 3.58–3.64 (m, 2H), 3.64–3.75 (m, 4H), 3.84 ppm (s, 2H); <sup>13</sup>C NMR (75 MHz, CDCl<sub>3</sub>): δ = 25.6, 42.6, 47.3, 66.5, 66.8, 165.7 ppm; ESI-MS: *m/z* calcd for C<sub>6</sub>H<sub>10</sub>BrNO<sub>2</sub>: 207.99677 [C<sub>6</sub>H<sub>10</sub>BrNO<sub>2</sub>+H]<sup>+</sup>; found: 207.99663.

**3-(2-Amino-3-(benzyloxy)benzyloxy)propan-1-ol (14)**: Compound **8** (1.4 g, 4.4 mmol) was taken up in acetic acid (21.0 mL). Iron powder (70 mesh) was then added to this solution and the contents were vigorously stirred at 50°C for 15 min. The yellow color of the heterogeneous mixture turned to dark brown. This was then filtered through celite pad and washed with ethyl acetate. The solvent was evaporated and the residue obtained was re-dissolved in ethyl acetate (200 mL) and extracted with water (3 × 200 mL). The organic layer collected was dried with anhydrous Na<sub>2</sub>SO<sub>4</sub> and was concentrated under vacuum. The residue obtained was purified by column chromatography using ethyl acetate/hexane (0.2:1) as the solvent mixture to obtain the product as white solid (1.0 g, 79%). <sup>1</sup>H NMR (300 MHz, CDCl<sub>3</sub>): δ = 1.78–1.87 (m, 2H), 3.58 (t, *J* = 6.04 Hz, 2H), 3.70 (t, *J* = 6.04 Hz, 2H), 4.55 (s, 2H), 5.07 (s, 2H), 6.64–6.72 (m, 1H), 6.73–6.80 (m, 1H), 6.86 (d, *J* = 7.93 Hz, 1H), 7.34–7.48 ppm (m, 5H); <sup>13</sup>C NMR (75 MHz, CDCl<sub>3</sub>): δ = 31.9, 60.1, 67.3, 70.3, 71.5, 111.7, 117.0, 122.1, 127.2, 127.7, 128.3, 135.6, 136.8, 146.3 ppm.

**Di-tert-butyl 2,2'-(2-(benzyloxy)-6-(3-hydroxypropoxy)methyl)phenylazanediyldiacetate (15)**: Compound **14** (3.7 g, 12.9 mmol), proton sponge (11.0 g, 51.6 mmol), and KI (0.2 g, 1.3 mmol) were taken up in MeCN (dry, 70 mL) and heated at reflux for 3 h. The RM was then cooled down and *tert*-butyl bromoacetate (7.5 mL, 51.6 mmol) was added to it. The contents were heated at reflux for 5 d. The RM was then filtered and evaporated. The residue obtained was re-dissolved in toluene and filtered again. The evaporated residue was then purified by column chromatography using ethyl acetate/hexane (0.3:1) as the solvent mixture to obtain the product (3.6 g, 54%) co-eluted with proton sponge (1.0 g). Some of the unused reactant was also recovered (0.7 g, 19%) at ethyl acetate/hexane (0.4–0.5:1) solvent mixture with traces of co-eluted proton sponge. <sup>1</sup>H NMR (300 MHz, CDCl<sub>3</sub>): δ = 1.41 (s, 18H), 1.82–1.95 (m, 2H), 3.77 (s, 8H), 4.93 (s, 2H), 5.10 (s, 2H), 6.87 (dd, *J* = 7.93, 1.51 Hz, 1H), 7.04–7.17 (m, 2H), 7.35–7.52 ppm (m, 5H); <sup>13</sup>C NMR (75 MHz, CDCl<sub>3</sub>): δ = 28.4, 32.6, 44.7, 57.9, 62.2, 69.9, 70.3, 70.6, 80.9, 112.2, 121.2, 125.8, 126.9, 127.7, 128.3, 128.9, 137.4, 137.5, 139.8, 156.9, 170.8 ppm; ESI-MS: *m/z* calcd for C<sub>29</sub>H<sub>41</sub>NO<sub>7</sub>: 538.29558 [C<sub>29</sub>H<sub>41</sub>NO<sub>7</sub>+Na]<sup>+</sup>; found: 538.29557.

**Di-tert-butyl 2,2'-(2-(benzyloxy)-6-(3-bromopropoxy)methyl)phenylazanediyldiacetate (16)**: Compound **15** (3.0 g, 5.8 mmol) and PPh<sub>3</sub> (3.0 g, 11.6 mmol) were dissolved in CH<sub>2</sub>Cl<sub>2</sub> (25 mL) and cooled to 0°C. CBr<sub>4</sub> (4.0 g, 12.2 mmol) was added in small portions. After complete addition, the RM was stirred at RT for 2 h. The solvent was evaporated and the

residue obtained was purified by column chromatography using ethyl acetate/hexane (0.05:1) as the solvent mixture to obtain the pure product as light-yellow oil (3.0 g, 88%). <sup>1</sup>H NMR (300 MHz, CDCl<sub>3</sub>): δ = 1.30 (s, 18H), 1.99–2.11 (m, 2H), 3.43 (t, *J* = 6.80 Hz, 2H), 3.56 (t, *J* = 5.85 Hz, 2H), 3.70 (s, 4H), 4.79 (s, 2H), 4.97 (s, 2H), 6.71–6.77 (m, 1H), 6.93–7.05 (m, 2H), 7.18–7.33 (m, 3H), 7.33–7.40 ppm (m, 2H); <sup>13</sup>C NMR (75 MHz, CDCl<sub>3</sub>): δ = 27.5, 30.2, 32.6, 56.9, 67.4, 69.2, 69.7, 79.8, 111.3, 120.3, 125.9, 126.8, 127.3, 128.0, 136.4, 138.9, 155.9, 169.8 ppm; ESI-MS: calcd for *m/z*: 600.19312 [C<sub>29</sub>H<sub>40</sub>BrNO<sub>6</sub>+Na]<sup>+</sup>; found: 600.19276.

**Tri-tert-butyl 2,2',2''-(10-(3-(3-(benzyloxy)-2-(bis(2-tert-butoxy-2-oxoethyl)amino)benzyloxy)propyl)-1,4,7,10-tetraazacyclododecane-1,4,7-triyl)triacetate (17)**: Tris-*tert*-Bu-DO3A (2.0 g, 4.0 mmol) and K<sub>2</sub>CO<sub>3</sub> (1.8 g, 13 mmol) were taken up in DMF (dry, 12 mL) and heated at 60°C for 1 h. The RM was brought to RT and compound **16** (3.0 g, 5.2 mmol) dissolved in DMF (5 mL) was added. The contents were heated at 60°C overnight. The RM was then filtered and concentrated under vacuum. The residue obtained was re-dissolved in CHCl<sub>3</sub> (300 mL) and washed with water (3 × 300 mL). The organic layer was dried under with Na<sub>2</sub>SO<sub>4</sub> and evaporated under vacuum to yellow oil. This was purified by column chromatography using MeOH/CH<sub>2</sub>Cl<sub>2</sub> (0.05:1) as the solvent mixture to obtain the pure product as light-yellow fluffy solid (2.2 g, 55%). <sup>1</sup>H NMR (300 MHz, CDCl<sub>3</sub>): δ = 1.30 (s, 18H), 1.33–1.42 (m, 27H), 1.62–1.75 (m, 2H), 2.14–2.51 (m, 11H), 2.61–2.94 (m, 7H), 2.94–3.20 (m, 6H), 3.45 (t, *J* = 5.85 Hz, 2H), 3.68 (s, 4H), 4.77 (s, 2H), 5.01 (s, 2H), 6.77 (dd, *J* = 7.93 Hz, 1H), 6.90–6.96 (m, 1H), 6.99–7.06 (m, 1H), 7.23–7.42 ppm (m, 5H); <sup>13</sup>C NMR (75 MHz, CDCl<sub>3</sub>): δ = 28.0, 28.17, 28.20, 50.5, 52.0, 53.7, 56.0, 56.7, 57.7, 69.1, 69.7, 70.4, 80.6, 82.6, 82.9, 111.7, 120.3, 126.7, 127.5, 128.1, 128.8, 136.9, 137.2, 139.9, 156.6, 170.5, 172.9, 173.7 ppm; ESI-MS: *m/z* calcd for C<sub>55</sub>H<sub>89</sub>N<sub>5</sub>O<sub>12</sub>: 506.83266 [C<sub>55</sub>H<sub>89</sub>N<sub>5</sub>O<sub>12</sub>+2H]<sup>2+</sup>; found: 506.83263.

**Tri-tert-butyl 2,2',2''-(10-(3-(2-(bis(2-tert-butoxy-2-oxoethyl)amino)-3-hydroxybenzyloxy)propyl)-1,4,7,10-tetraazacyclododecane-1,4,7-triyl)triacetate (18)**: Compound **17** (2.2 g, 2.1 mmol) was dissolved in ethanol (dry, 10 mL). [Pd(OH)<sub>2</sub>] (50% wet, 10% w/w) was suspended and the heterogeneous mixture was stirred in a Parr apparatus under H<sub>2</sub> atmosphere (3 atm) for 5 h. The RM was then filtered and the solvent was evaporated to obtain the product as yellow solid (1.8 g, 95%). <sup>1</sup>H NMR (300 MHz, CDCl<sub>3</sub>): δ = 1.20 (brs, 45H), 1.53 (brs, 1H), 1.84 (brs, 1H), 2.00–2.37 (m, 5H), 2.43–2.72 (m, 8H), 2.75–3.02 (m, 6H), 3.07 (s, 2H), 3.20–3.35 (m, 4H), 3.37–3.66 (m, 7H), 4.31–4.46 (m, 2H), 6.55–6.70 (m, 2H), 6.77–6.92 ppm (m, 1H); <sup>13</sup>C NMR (75 MHz, CDCl<sub>3</sub>): δ = 27.6, 27.7, 27.8, 27.9, 31.0, 47.5, 49.8, 50.1, 50.4, 51.9, 52.3, 52.7, 54.9, 55.5, 56.1, 56.2, 56.3, 56.7, 67.0, 67.6, 68.9, 69.4, 69.5, 81.4, 81.9, 82.2, 82.5, 116.4, 119.9, 120.1, 127.3, 127.4, 135.3, 137.8, 138.0, 155.0, 169.7, 170.1, 172.3, 172.5, 173.2 ppm; ESI-MS: *m/z* calcd for C<sub>48</sub>H<sub>83</sub>N<sub>5</sub>O<sub>12</sub>: 461.80919 [C<sub>48</sub>H<sub>83</sub>N<sub>5</sub>O<sub>12</sub>+2H]<sup>2+</sup>; found: 461.80924.

**Tri-tert-butyl 2,2',2''-(10-(3-(2-(bis(2-tert-butoxy-2-oxoethyl)amino)-3-(2-morpholino-2-oxoethoxy)benzyloxy)propyl)-1,4,7,10-tetraazacyclododecane-1,4,7-triyl)triacetate (20)**: NaH (0.02 g, 0.54 mmol, 60% emulsion in oil) was suspended in freshly distilled THF (5 mL) and cooled down to –5°C. After 15 min, compound **18** (0.5 g, 0.54 mmol) dissolved in a minimum amount of THF (dry, ca. 2 mL) was added. The RM was stirred for 20 min and compound **19** (0.45 g, 2.2 mmol) was added to it while the temperature was maintained at –5°C. After 5 min, NaH (0.02 g, 0.54 mmol) was again added and the RM was finally stirred at the same temperature for another 30 min. The completion of reaction was monitored by ESI-MS. The reaction was quenched by addition of water. The product was extracted in CHCl<sub>3</sub> from the reaction mixture, the organic layer was dried with anhydrous Na<sub>2</sub>SO<sub>4</sub> and evaporated to a yellow oil. This was purified by column chromatography using MeOH/CH<sub>2</sub>Cl<sub>2</sub> (0.08–0.1:1) as the solvent mixture to obtain the product (0.35 g, 62%). <sup>1</sup>H NMR (300 MHz, CDCl<sub>3</sub>): δ = 1.32 (s, 18H), 1.34–1.42 (m, 27H), 1.61–1.75 (m, 2H), 2.18–2.50 (m, 9H), 2.65–2.91 (m, 5H), 2.97–3.18 (m, 5H), 3.40–3.47 (m, 2H), 3.48–3.53 (m, 2H), 3.54–3.68 (m, 11H), 3.72 (s, 4H), 4.71 (s, 2H), 4.76 (s, 2H), 6.80 (d, *J* = 7.93 Hz, 1H), 6.95 (d, *J* = 7.55 Hz, 1H), 7.03 ppm (t, *J* = 7.74 Hz, 1H); <sup>13</sup>C NMR (75 MHz, CDCl<sub>3</sub>): δ = 26.7, 27.7, 27.87, 27.98, 42.1, 45.5, 50.2, 50.7, 51.8, 53.4, 55.7, 56.4, 57.1, 66.6, 66.7, 67.4, 68.8, 69.3, 80.3, 82.3, 82.7, 112.0, 120.9, 126.3, 136.9, 139.2,

155.6, 166.5, 170.2, 172.5 ppm; ESI-MS:  $m/z$  calcd for  $C_{54}H_{92}N_6O_{14}$ : 1071.7 [ $C_{54}H_{92}N_6O_{14} + Na$ ] $^+$ ; found: 1071.8.

**2,2',2''-(10-(3-(2-(Bis(carboxymethyl)amino)-3-(2-morpholino-2-oxoethoxy)benzyloxy)propyl)-1,4,7,10-tetraazacyclododecane-1,4,7-triyl)triacetic acid (21)**: Compound **20** (0.3 g, 0.28 mmol) was dissolved in a minimum amount of  $CH_2Cl_2$  (ca. 1 mL) and TFA (15 mL) added to it. The RM was stirred at RT overnight. TFA was evaporated under vacuum and the residue obtained was purified by RP-HPLC to obtain the pure product (0.14 g, 65%).  $^1H$  NMR (300 MHz,  $D_2O$ ):  $\delta$  = 1.88 (brs, 2H), 2.77–3.03 (m, 8H), 3.12–3.19 (m, 4H), 3.20–3.33 (m, 6H), 3.34–3.44 (m, 6H), 3.46–3.63 (m, 8H), 3.67 (s, 2H), 3.94 (s, 4H), 4.62 (s, 2H), 4.88 (s, 2H), 6.81 (dd,  $J$  = 7.46, 4.44 Hz, 2H), 7.12 ppm (t,  $J$  = 7.84 Hz, 1H);  $^{13}C$  NMR (75 MHz,  $D_2O$ ):  $\delta$  = 21.9, 41.3, 44.0, 47.6, 48.8, 50.4, 50.9, 52.6, 55.3, 58.8, 64.8, 65.2, 65.4, 66.9, 69.6, 112.9, 121.9, 128.4, 133.1, 134.3, 152.9, 165.4, 169.1, 173.4, 173.9 ppm; ESI-MS:  $m/z$  calcd for  $C_{34}H_{52}N_6O_{14}$ : 383.16980 [ $C_{34}H_{52}N_6O_{14} - H$ ] $^-$ ; found: 383.16981.

**Ethyl 2-(2-bromoethoxy)acetate (22)**: Bromoethanol (2.1 mL, 30.2 mmol) was taken up in  $CH_2Cl_2$  (50 mL). Rhodium(II) acetate dimer powder (0.15 g, 0.33 mmol) was added under ice. After 5 min, the ice bath was removed and ethyl diazoacetate (3.5 mL, 33.2 mmol) dissolved in  $CH_2Cl_2$  (25 mL) was added dropwise to it. After complete addition, the RM was stirred for another 2 h. It was then filtered through a celite pad and the filtrate was concentrated under vacuum. The residue obtained was purified by column chromatography using ethyl acetate/hexane (0.05–0.1:1) to obtain the product as transparent oil (4.7 g, 75%).  $^1H$  NMR (300 MHz,  $CDCl_3$ ):  $\delta$  = 1.24 (t,  $J$  = 7.18 Hz, 3H), 3.47 (t,  $J$  = 6.23 Hz, 2H), 3.85 (t,  $J$  = 6.23 Hz, 2H), 4.10 (s, 2H), 4.18 ppm (q,  $J$  = 14.16, 7.18 Hz, 2H);  $^{13}C$  NMR (75 MHz,  $CDCl_3$ ):  $\delta$  = 14.1, 29.9, 60.9, 68.4, 71.4, 170.0 ppm; ESI-MS:  $m/z$  calcd for  $C_6H_{11}BrO_3$ : 232.97838 [ $C_6H_{11}BrO_3 + Na$ ] $^+$ ; found: 232.97834.

**2,2',2''-(10-(3-(2-(Bis(carboxymethyl)amino)-3-(2-(carboxymethoxy)ethoxy)benzyloxy)propyl)-1,4,7,10-tetraazacyclododecane-1,4,7-triyl)triacetic acid (24)**: NaH (0.012 g, 0.3 mmol, 60% emulsion in oil) was taken in freshly distilled THF (5 mL) and cooled down to  $-5^\circ C$ . After 15 min, compound **18** (0.28 g, 0.3 mmol) dissolved in minimum amount of THF (dry, ca. 0.5 mL) was added to it. The reaction mixture was stirred for 20 min and compound **22** (0.45 g, 1.2 mmol) was added to it while the temperature was maintained at  $-5^\circ C$ . After 5 min, NaH (0.02 g, 0.54 mmol) was again added to it and the RM was finally stirred at the same temperature for another hour. The completion of reaction was monitored by ESI-MS. The reaction was quenched by addition of water. The solvent was evaporated under vacuum and the contents were re-dissolved in a small amount of  $CH_2Cl_2$  and cooled down under ice-salt bath. HBr/AcOH (5 mL) was added to it and the RM was stirred at RT for 5 h. The acid was evaporated under vacuum. The residue obtained was re-dissolved in water and the pH was increased to 7 by 1 N NaOH. This was then purified by RP-HPLC to obtain the product as transparent solid (0.057 g, 25%).  $^1H$  NMR (300 MHz,  $D_2O$ ):  $\delta$  = 1.94 (brs, 2H), 2.96 (s, 8H), 3.13–3.26 (m, 6H), 3.26–3.33 (m, 4H), 3.34–3.40 (m, 2H), 3.40–3.48 (m, 2H), 3.54–3.63 (m, 3H), 3.73 (brs, 2H), 3.86–3.93 (m, 2H), 4.01–4.10 (m, 3H), 4.14 (s, 2H), 4.16–4.22 (m, 2H), 4.72 (s, 2H), 6.84 (d,  $J$  = 7.36 Hz, 1H), 7.01 (d,  $J$  = 8.31 Hz, 1H), 7.23 ppm (t,  $J$  = 7.84 Hz, 1H);  $^{13}C$  NMR (75 MHz,  $CDCl_3$ ):  $\delta$  = 22.8, 48.4, 48.5, 49.7, 51.3, 51.8, 53.4, 56.2, 59.7, 67.6, 67.9, 69.4, 70.8, 114.3, 122.1, 130.1, 131.8, 133.8, 153.4, 173.4, 174.3, 174.6 ppm; ESI-MS:  $m/z$  calcd for  $C_{32}H_{49}N_5O_{15}$  (compound **23**): [ $C_{32}H_{49}N_5O_{15} - H$ ] $^-$ : 370.65398; found: 370.65416; ESI-MS:  $m/z$  calcd for  $C_{54}H_{93}N_5O_{15}$  (compound **24**): 1052.7 [ $C_{54}H_{93}N_5O_{15} + H$ ] $^+$ ; found: 1052.9.

General procedure for preparation of  $Ln^{III}$  complexes: The  $Ln^{III}$  complexes of DOPTRA ligands were prepared by adding 1.1 equiv of  $LnCl_3$  solution of known concentration. The reaction was kept for stirring at  $50^\circ C$  and the pH was maintained at 7 with the addition of 1 M NaOH solution. The RM was then kept for stirring at the same temperature overnight. Chelex 100 was added to the RM and the reaction was allowed to stir at RT for another 1 h. The absence of free  $Ln^{3+}$  was checked by xylenol orange indicator in HCl/urotropine buffer (pH 5.5). It was then filtered and the water evaporated under vacuum to obtain the complex as solid. This was further purified by sephadex LH-20 column (13  $\times$  2.5 cm

for  $\approx 50$ –150 mg). The product was eluted with pure water without application of pressure from top. The fractions collected were analyzed by ESI-MS. The desired fractions were mixed and the water was evaporated to obtain the  $Ln^{III}$  complex. For each  $Ln$ –L sample the final concentrations were determined by ICP-OES.

**ESI-MS of Gd-DOPTRA-2**:  $m/z$  calcd for  $C_{27}H_{36}GdN_5O_{13}$ : 794.4 [ $C_{27}H_{36}GdN_5O_{13} - H$ ] $^-$ ; found: 794.2 [ $M - H$ ] $^-$ , 817.2 [ $M - H + Na$ ] $^-$  with appropriate isotopic distribution for  $Gd^{3+}$ .

**ESI-MS of Tb-DOPTRA-2**:  $m/z$  calcd for  $C_{27}H_{36}TbN_5O_{13}$ : 797.1 [ $C_{27}H_{36}TbN_5O_{13} - H$ ] $^-$ ; found: 797.0 [ $M - H$ ] $^-$  with appropriate isotopic distribution for  $Tb^{3+}$ .

**ESI-MS of Gd-DOPTRA-3**:  $m/z$  calcd for  $C_{30}H_{42}GdN_5O_{14}$ : 852.6 [ $C_{30}H_{42}GdN_5O_{14} - H$ ] $^-$ ; found: 853.2 [ $M - H$ ] $^-$ , 875.1 [ $M - H + Na$ ] $^-$  with appropriate isotopic distribution for  $Gd^{3+}$ .

**ESI-MS of Tb-DOPTRA-3**:  $m/z$  calcd for  $C_{30}H_{42}TbN_5O_{14}$ : 854.2 [ $C_{30}H_{42}TbN_5O_{14} - H$ ] $^-$ ; found: 854.0 [ $M - H$ ] $^-$  with appropriate isotopic distribution for  $Tb^{3+}$ .

**ESI-MS of Gd-DOPTRA-4**:  $m/z$  calcd for  $C_{34}H_{49}GdN_6O_{14}$ : 922.2 [ $C_{34}H_{49}GdN_6O_{14} + H$ ] $^+$ ; found: 922.3 with appropriate isotopic distribution for  $Gd^{3+}$ .

**ESI-MS of Tb-DOPTRA-4**:  $m/z$  calcd for  $C_{34}H_{49}TbN_6O_{14}$ : 923.2 [ $C_{34}H_{49}TbN_6O_{14} - H$ ] $^-$ ; found: 923.0 with appropriate isotopic distribution for  $Tb^{3+}$ .

**ESI-MS of Gd-DOPTRA-5**:  $m/z$  calcd for  $C_{32}H_{46}GdN_5O_{15}$ : 897.2 [ $C_{32}H_{46}GdN_5O_{15} + H$ ] $^+$ ; found: 897.3 with appropriate isotopic distribution for  $Gd^{3+}$ .

**ESI-MS of Tb-DOPTRA-5**:  $m/z$  calcd for  $C_{32}H_{46}TbN_5O_{15}$ : 898.2 [ $C_{32}H_{46}TbN_5O_{15} - H$ ] $^-$ ; found: 898.0 with isotopic distribution for  $Tb^{3+}$ .

## Acknowledgements

The authors would like to thank the Max Planck Society for financial support. The work in France was supported by La Ligue contre le Cancer. This work was carried out in the framework of the COST D38 Action "Metal Based Systems for Molecular Imaging" and COST actions TD1004 and CM1006. S.P. acknowledges support from the Institut National de la Santé et de la Recherche Médicale (INSERM). M.B. thanks the Ministero dell' Istruzione, dell' Università e della Ricerca (MIUR; project PRIN 2009) for financial support.

- [1] a) L. R. Squire, D. Berg, F. E. Bloom, S. du Lac, A. Ghosh, N. C. Spitzer, L. Bloom, S. McConnell, J. L. Roberts, M. Zigmond, *Fundamental Neuroscience*, Academic Press, New York, **2003**; b) M. J. Beridge, M. D. Bootman, H. L. Roderick, *Nat. Rev. Mol. Cell Biol.* **2003**, *4*, 517–529; c) S. Govoni, M. Amadio, F. Battaini, A. Pascale, *Curr Pharm Des* **2010**, *16*, 660–671.
- [2] a) M. Brini, E. Carafoli, *Cell. Mol. Life Sci.* **2000**, *57*, 354–370; b) J. Q. Zheng, M. M. Poo, *Annu Rev Cell Dev Biol* **2007**, *23*, 375–404; c) I. Bezprozvanny, M. P. Mattson, *Trends Neurosci.* **2008**, *31*, 454–463.
- [3] D. M. Egelman, P. R. Montague, *J. Neurosci.* **1998**, *18*, 8580–8589.
- [4] a) C. Nicholson, *Fed. Proc.* **1980**, *39*, 1519–1523; b) M. Erecińska, I. A. Silver, *Prog. Neurobiol.* **1994**, *43*, 37–71; c) C. Nicholson, G. T. Bruggencate, R. Steinberg, H. Stockle, *Proc. Natl. Acad. Sci. USA* **1977**, *74*, 1287–1290.
- [5] a) Y. Okubo, K. Kanemaru, M. Iino, *Antioxid. Redox Signaling* **2011**, *14*, 1303–1314; b) A. Sarma, W. Yang, *Protein Cell* **2011**, *2*, 291–302; c) R. Y. Tsien, *Soc. Gen. Physiol. Ser.* **1986**, *40*, 327–345; d) C. C. Ashley, J. D. Potter, P. Strang, J. Godber, A. Walton, P. J. Griffiths, *Cell Calcium* **1985**, *6*, 159–181.
- [6] A. E. Merbach, E. Toth, in *The Chemistry of Contrast Agents in Medical Magnetic Resonance Imaging*, Wiley, Chichester, **2001**.
- [7] a) K. Dhingra, P. Fouskova, G. Angelovski, M. E. Maier, N. K. Logothetis, E. Toth, *J. Biol. Inorg. Chem.* **2007**, *13*, 35–46; b) K. Dhingra,

- ra, M. E. Maier, M. Beyerlein, G. Angelovski, N. K. Logothetis, *Chem. Commun.* **2008**, 3444–3446; c) W.-H. Li, S. E. Fraser, T. J. Meade, *J. Am. Chem. Soc.* **1999**, *121*, 1413; d) E. L. Que, E. Gianolio, S. L. Baker, A. P. Wong, S. Aime, C. J. Chang, *J. Am. Chem. Soc.* **2009**, *131*, 8527–8536; e) J. L. Major, G. Parigi, C. Luchinat, T. J. Meade, *Proc. Natl. Acad. Sci. USA* **2007**, *104*, 13881–13886.
- [8] L. M. Urbanczyk-Pearson, T. J. Meade, *Nat. Protoc.* **2008**, *3*, 341–350.
- [9] E. L. Que, C. J. Chang, *J. Am. Chem. Soc.* **2006**, *128*, 15942–15943.
- [10] O. Tour, S. R. Adams, R. A. Kerr, R. M. Meijer, T. J. Sejnowski, R. W. Tsien, R. Y. Tsien, *Nat. Chem. Biol.* **2007**, *3*, 423–431.
- [11] R. H. E. Hudson, M. Suchy, *Eur. J. Org. Chem.* **2008**, *2008*, 4847.
- [12] M. Lutz, J. Pursiainen, R. Aksela, *Z. Naturforsch.* **2005**, *60b*, 408–412.
- [13] a) S. Aime, M. Botta, E. Terreno, *Adv. Inorg. Chem.* **2005**, *57*, 173–237; b) P. Caravan, *Acc. Chem. Res.* **2009**, *42*, 851–862.
- [14] a. Beeby, I. M. Clarkson, R. Dickins, s. Faulkner, D. Parker, L. Royle, A. S. de Sousa, J. A. G. Williams, M. Woods, *J. Chem. Soc. Perkin Trans. 2* **1999**, 493–504.
- [15] a) M. Botta, *Eur. J. Inorg. Chem.* **2000**, 399–407; b) A. Mishra, N. K. Logothetis, D. Parker, *Chem. Eur. J.* **2011**, *17*, 1529–1537.
- [16] a) L. Helm, G. M. Nicolle, A. E. Merbach, *Adv. Inorg. Chem.* **2005**, *57*, 327–379; b) H. D. Powell, O. M. Ni Dhubghaill, D. Pubanz, L. Helm, Y. S. Lebedev, W. Schlaepfer, A. E. Merbach, *J. Am. Chem. Soc.* **1996**, *118*, 9333–9346.
- [17] L. Tei, G. Gugliotta, Z. Baranyai, M. Botta, *Dalton Trans.* **2009**, 9712–9714.
- [18] S. Aime, A. Barge, A. Borel, M. Botta, S. Chemerisov, A. E. Merbach, U. Müller, D. Pubanz, *Inorg. Chem.* **1997**, *36*, 5104–5112.
- [19] S. Aime, I. M. Botta, F. Fedeli, E. Gianolio, E. Terreno, P. Anelli, *Chem. Eur. J.* **2001**, *7*, 5261–5269.
- [20] a) V. Jacques, S. Dumas, W. C. Sun, J. S. Troughton, M. T. Greenfield, P. Caravan, *Invest. Radiol.* **2010**, *45*, 613–624; b) P. Lebduskova, P. Hermann, L. Helm, E. Toth, J. Kotek, K. Binnemans, J. Rudovsky, I. Lukes, A. E. Merbach, *Dalton Trans.* **2007**, 493–501.
- [21] a) J. Rudovsky, P. Cigler, J. Kotek, P. Hermann, P. Vojtisek, I. Lukes, J. A. Peters, L. Vander Elst, R. N. Muller, *Chem. Eur. J.* **2005**, *11*, 2373–2384; b) S. Aime, M. Botta, S. G. Crich, G. Giovenzana, R. Pagliarin, M. Sisti, E. Terreno, *Magn. Reson. Chem.* **1998**, *36*, S200–S208; c) M. P. Placidi, M. Botta, F. K. Kálmán, G. E. Hagberg, Z. Baranyai, A. Krenzer, A. K. Rogerson, E. Tóth, N. K. Logothetis, G. Angelovski, *Chem. Eur. J.* **2013**, *19*, 11644–11660.
- [22] a) P. Lebduskova, P. Hermann, L. Helm, E. Toth, J. Kotek, K. Binnemans, J. Rudovsky, I. Lukes, A. E. Merbach, *Dalton Trans.* **2007**, 493–501; b) J. Rudovsky, P. Cigler, J. Kotek, P. Hermann, P. Vojtisek, I. Lukes, J. A. Peters, L. Vander Elst, R. N. Muller, *Chem. Eur. J.* **2005**, *11*, 2373–2384; c) S. Aime, M. Botta, S. G. Crich, G. Giovenzana, R. Pagliarin, M. Sisti, E. Terreno, *Magn. Reson. Chem.* **1998**, *36*, S200–S208.
- [23] a) Z. Jaszberenyi, A. Sour, E. Toth, M. Benmelouka, A. E. Merbach, *Dalton Trans.* **2005**, 2713–2719; b) R. Ruloff, E. Toth, R. Scopelliti, R. Tripier, H. Handel, A. E. Merbach, *Chem. Commun.* **2002**, 2630–2631.
- [24] Y. Yamaguchi, *Cell. Mol. Life Sci.* **2000**, *57*, 276–289.

Received: January 17, 2013

Revised: August 25, 2013

Published online: November 7, 2013